CERN/LHCC 2012-007
LHCb TDR 12
25 May 2012

Framework TDR

LHCb UPGRADE

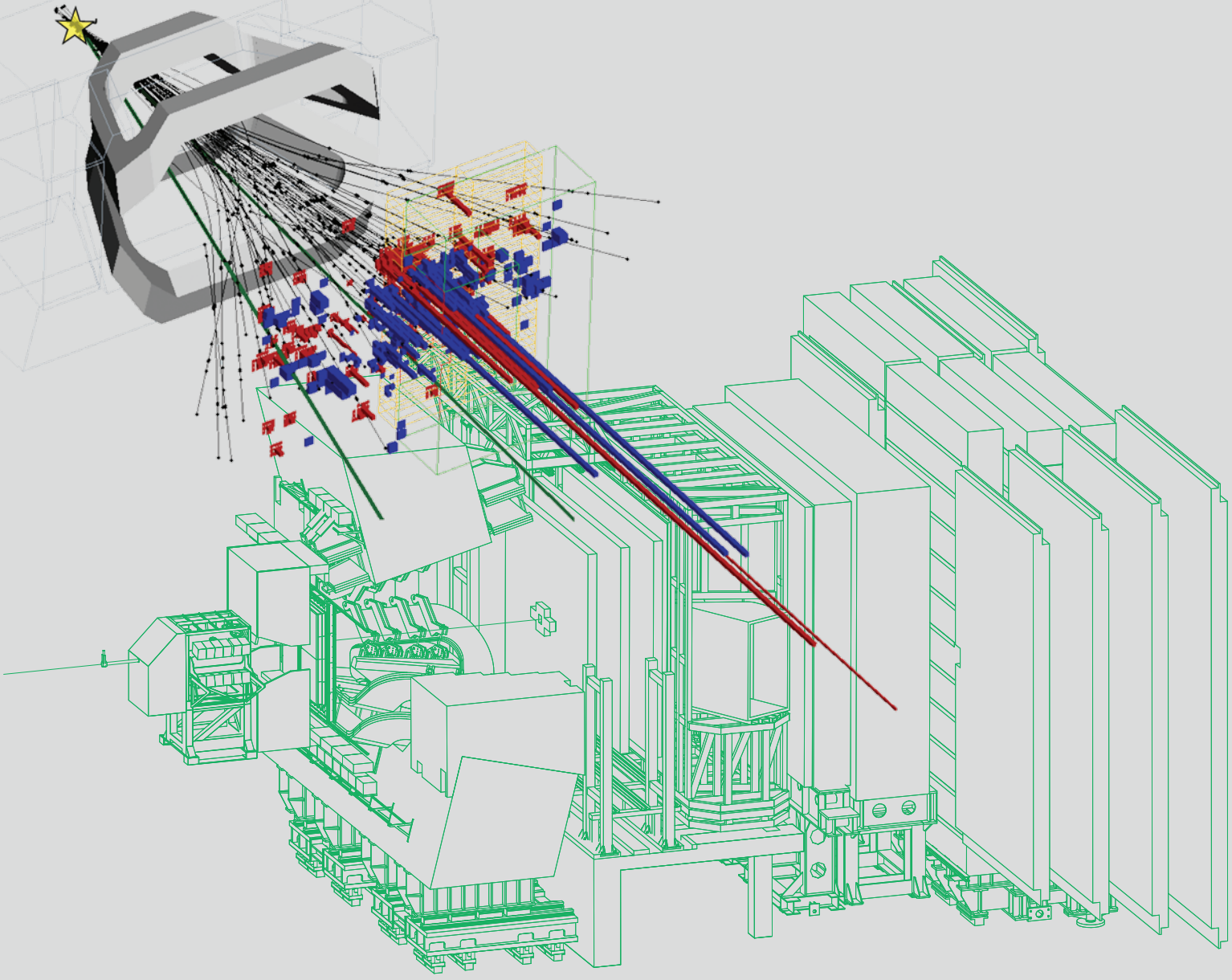

Technical Design Report

CERN/LHCC 2012-007
LHCb TDR 12
25 May 2012

Framework TDR for the LHCb upgrade

The LHCb Collaboration

Abstract

This document is a Framework Technical Design Report for the upgrade of the LHCb experiment. It adds to the information in the Letter of Intent, in particular concerning the foreseen schedule, cost and participating institutes. Updates are given for the physics performance, based on the experience gained with the first full year of data taking, on the detector requirements and the progress of the sub-system R&D. Within the framework presented here, it is expected that the individual sub-system TDRs will follow on completion of the R&D phase in the next year.

The LHCb collaboration

I. Bediaga[1], J.M. De Miranda[1], F. Ferreira Rodrigues[1], J. Magnin[1], A. Massafferri[1], I. Nasteva[1], A.C. dos Reis[1]
[1] *Centro Brasileiro de Pesquisas Físicas (CBPF), Rio de Janeiro, Brazil*

S. Amato[2], K. Carvalho Akiba[2], L. De Paula[2], O. Francisco[2], M. Gandelman[2], A. Gomes[2], J.H. Lopes[2], J.M. Otalora Goicochea[2], E. Polycarpo[2], M.S. Rangel[2], B. Souza De Paula[2], D. Vieira[2]
[2] *Universidade Federal do Rio de Janeiro (UFRJ), Rio de Janeiro, Brazil*

C. Göbel[3], J. Molina Rodriguez[3]
[3] *Pontifícia Universidade Católica do Rio de Janeiro (PUC-Rio), Rio de Janeiro, Brazil*

P. Chen[4,39], Y. Gao[4], G. Gong[4], H. Gong[4], F. Jing[4], L. Li[4], Y. Li[4], B. Liu[4], H. Lu[4], B. Shao[4], S. Wu[4], T. Xue[4], Z. Yang[4], X. Yuan[4], M. Zeng[4], F. Zhang[4], Y. Zhang[4], L. Zhong[4]
[4] *Center for High Energy Physics, Tsinghua University, Beijing, China*

I. De Bonis[5], D. Decamp[5], C. Drancourt[5], Ph. Ghez[5], P. Hopchev[5], J.-P. Lees[5], I.V. Machikhiliyan[5,31], M.-N. Minard[5], B. Pietrzyk[5], S. T'Jampens[5], V. Tisserand[5], E. Tournefier[5,53], G. Vouters[5]
[5] *LAPP, Université de Savoie, CNRS/IN2P3, Annecy-Le-Vieux, France*

Z. Ajaltouni[6], H. Chanal[6], E. Cogneras[6], O. Deschamps[6], I. El Rifai[6], P. Henrard[6], M. Hoballah[6], M. Jahjah Hussein[6], R. Lefèvre[6], L. Li Gioi[6], S. Monteil[6], V. Niess[6], P. Perret[6], D.A. Roa Romero[6], K. Sobczak[6]
[6] *Clermont Université, Université Blaise Pascal, CNRS/IN2P3, LPC, Clermont-Ferrand, France*

C. Adrover[7], E. Aslanides[7], J.-P. Cachemiche[7], J. Cogan[7], P.-Y. Duval[7], F. Hachon[7], B. Khanji[7], R. Le Gac[7], O. Leroy[7], G. Mancinelli[7], E. Maurice[7], M. Perrin-Terrin[7], F. Rethore[7], M. Sapunov[7], J. Serrano[7], A. Tsaregorodtsev[7]
[7] *CPPM, Aix-Marseille Université, CNRS/IN2P3, Marseille, France*

S. Barsuk[8], C. Beigbeder-Beau[8], T. Cacérès[8], O. Callot[8], D. Charlet[8], O. Duarte[8], J. He[8], B. Jean-Marie[8], O. Kochebina[8], J. Lefrançois[8], F. Machefert[8], A. Martín Sánchez[8], M. Nicol[8], P. Robbe[8], M.-H. Schune[8], M. Teklishyn[8], V. Tocut[8], B. Viaud[8], I. Videau[8]
[8] *LAL, Université Paris-Sud, CNRS/IN2P3, Orsay, France*

E. Ben-Haim[9], M. Benayoun[9], P. David[9], L. Del Buono[9], A. Martens[9], F. Polci[9]
[9] *LPNHE, Université Pierre et Marie Curie, Université Paris Diderot, CNRS/IN2P3, Paris, France*

T. Brambach[10], Ch. Cauet[10], M. Deckenhoff[10], M. Domke[10], R. Ekelhof[10], M. Kaballo[10], T.M. Karbach[10], F. Kruse[10], J. Merkel[10], K. Rudloff[10], S. Schleich[10], M. Schlupp[10], B. Spaan[10], S. Swientek[10], K. Warda[10], J. Wishahi[10]
[10] *Fakultät Physik, Technische Universität Dortmund, Dortmund, Germany*

C. Bauer[11], M. Britsch[11], C. Föhr[11], M. Fontana[11], H. Fuchs[11], W. Hofmann[11], T. Kihm[11],

D. Popov[11], M. Schmelling[11], D. Volyanskyy[11], H. Voss[11], M. Zavertyaev[11,a]
[11] *Max-Planck-Institut für Kernphysik (MPIK), Heidelberg, Germany*

S. Bachmann[12], A. Bien[12], J. Blouw[12], F. Dordei[12], C. Färber[12], E. Gersabeck[12], S. Hansmann-Menzemer[12], A. Jaeger[12], K. Kreplin[12], G. Krocker[12], C. Linn[12], J. Marks[12], M. Meissner[12], T. Nikodem[12], P. Seyfert[12], S. Stahl[12], J. van Tilburg[12], U. Uwer[12], S. Wandernoth[12], D. Wiedner[12], A. Zhelezov[12]
[12] *Physikalisches Institut, Ruprecht-Karls-Universität Heidelberg, Heidelberg, Germany*

O. Grünberg[13], T. Hartmann[13], C. Voß[13], R. Waldi[13]
[13] *Institut für Physik, Universität Rostock, Rostock, Germany*

S. Bifani[14], S. Farry[14], P. Ilten[14], T. Kechadi[14], Z. Mathe[14], R. McNulty[14], R. Wallace[14], W.C. Zhang[14]
[14] *School of Physics, University College Dublin, Dublin, Ireland*

D.A. Milanes[15], A. Palano[15,b]
[15] *Sezione INFN di Bari, Bari, Italy*

A. Carbone[16,c], I. D'Antone[16], D. Derkach[16,38], A. Falabella[16,e], D. Galli[16,c], I. Lax[16], U. Marconi[16], S. Perazzini[16,c], V. Vagnoni[16], G. Valenti[16], M. Zangoli[16]
[16] *Sezione INFN di Bologna, Bologna, Italy*

W. Bonivento[17], S. Cadeddu[17], A. Cardini[17], A. Lai[17], G. Manca[17,d], R. Oldeman[17,d,38], B. Saitta[17,d]
[17] *Sezione INFN di Cagliari, Cagliari, Italy*

W. Baldini[18], C. Bozzi[18], F. Evangelisti[18], L. Landi[18,e], A. Mazurov[18,33,38], M. Savrie[18,e], S. Squerzanti[18], S. Vecchi[18]
[18] *Sezione INFN di Ferrara, Ferrara, Italy*

A. Bizzeti[19,h], M. Frosini[19,f], G. Graziani[19], G. Passaleva[19], M. Veltri[19,g]
[19] *Sezione INFN di Firenze, Firenze, Italy*

M. Anelli[20], F. Archilli[20,38], G. Bencivenni[20], P. Campana[20,38], P. Ciambrone[20], P. De Simone[20], G. Felici[20], G. Lanfranchi[20,38], M. Palutan[20], A. Saputi[20], A. Sarti[20,l], B. Sciascia[20], F. Soomro[20,38]
[20] *Laboratori Nazionali dell'INFN di Frascati, Frascati, Italy*

R. Cardinale[21,i,38], F. Fontanelli[21,i], C. Patrignani[21,i], A. Petrolini[21,i]
[21] *Sezione INFN di Genova, Genova, Italy*

M. Calvi[22,j], S. Furcas[22], A. Giachero[22], C. Gotti[22], M. Kucharczyk[22,26,38,j], M. Maino[22], C. Matteuzzi[22], G. Pessina[22]
[22] *Sezione INFN di Milano Bicocca, Milano, Italy*

G. Carboni[23,k], S. De Capua[23,k], G. Sabatino[23,k], E. Santovetti[23,k], A. Satta[23]
[23] *Sezione INFN di Roma Tor Vergata, Roma, Italy*

A.A. Alves Jr[24], G. Auriemma[24,m], V. Bocci[24], G. Martellotti[24], G. Penso[24,l], D. Pinci[24],

R. Santacesaria[24], C. Satriano[24,m], A. Sciubba[24]
[24] *Sezione INFN di Roma La Sapienza, Roma, Italy*

S. Nisar[25]
[25] *Institute of Information Technology, COMSATS, Lahore, Pakistan*

P. Morawski[26], G. Polok[26], M. Witek[26]
[26] *Henryk Niewodniczanski Institute of Nuclear Physics Polish Academy of Sciences, Kraków, Poland*

B. Muryn[27], A. Oblakowska-Mucha[27], K. Senderowska[27], T. Szumlak[27]
[27] *AGH University of Science and Technology, Kraków, Poland*

Z. Guzik[28], A. Nawrot[28], M. Szczekowski[28], A. Ukleja[28]
[28] *Soltan Institute for Nuclear Studies, Warsaw, Poland*

I. Burducea[29], C. Coca[29], M. Dogaru[29], A. Grecu[29], F. Maciuc[29], R. Muresan[29], M. Orlandea[29], C. Pavel-Nicorescu[29], B. Popovici[29], S. Stoica[29], M. Straticiuc[29], E. Teodorescu[29]
[29] *Horia Hulubei National Institute of Physics and Nuclear Engineering, Bucharest-Magurele, Romania*

G. Alkhazov[30], B. Bochin[30], N. Bondar[30], A. Dzyuba[30], S. Gets[30], V. Golovtsov[30], A. Kashchuk[30], O. Maev[30,38], M. Matveev[30], N. Sagidova[30], Y. Shcheglov[30], S. Volkov[30], A. Vorobyev[30]
[30] *Petersburg Nuclear Physics Institute (PNPI), Gatchina, Russia*

V. Balagura[31], S. Belogurov[31], I. Belyaev[31], V. Egorychev[31], D. Golubkov[31], T. Kvaratskheliya[31,38], D. Savrina[31], A. Semennikov[31], P. Shatalov[31], V. Shevchenko[31], A. Zhokhov[31]
[31] *Institute of Theoretical and Experimental Physics (ITEP), Moscow, Russia*

A. Berezhnoy[32], G. Bogdanova[32], I. Komarov[32], M. Korolev[32], A. Leflat[32,38], N. Nikitin[32], V. Volkov[32], E. Zverev[32]
[32] *Institute of Nuclear Physics, Moscow State University (SINP MSU), Moscow, Russia*

S. Filippov[33], E. Gushchin[33], O. Karavichev[33], L. Kravchuk[33], Y. Kudenko[33], S. Laptev[33], A. Tikhonov[33]
[33] *Institute for Nuclear Research of the Russian Academy of Sciences (INR RAN), Moscow, Russia*

A. Bondar[34], S. Eidelman[34], P. Krokovny[34], V. Kudryavtsev[34], L. Shekhtman[34], V. Vorobyev[34]
[34] *Budker Institute of Nuclear Physics (SB RAS) and Novosibirsk State University, Novosibirsk, Russia*

A. Artamonov [35], K. Belous[35], R. Dzhelyadin[35], Yu. Guz[35], A. Novoselov[35], V. Obraztsov[35], A. Ostankov[35], V. Romanovsky[35], M. Shapkin[35], O. Stenyakin[35], O. Yushchenko[35]
[35] *Institute for High Energy Physics (IHEP), Protvino, Russia*

C. Abellan Beteta[36,n], M. Calvo Gomez[36,n], A. Camboni[36], A. Casajus Ramo[36], A. Comerma-Montells[36], F. Domingo Bonal[36,n], L. Garrido[36], D. Gascon[36], M. Grabalosa Gándara[36], R. Graciani Diaz[36], E. Graugés[36], E. Lopez Asamar[36], J. Mauricio[36], V. Mendez-Munoz[36,o], A. Pérez-Calero Yzquierdo[36], E. Picatoste Olloqui[36], B. Pie Valls[36], C. Potterat[36], A. Puig Navarro[36], M. Rosello[36,n], H. Ruiz[36], R. Vazquez Gomez[36], X. Vilasis-Cardona[36,n]
[36] *Universitat de Barcelona, Barcelona, Spain*

B. Adeva[37], P. Alvarez Cartelle[37], X. Cid Vidal[37], A. Dosil Suárez[37], D. Esperante Pereira[37], V. Fernandez Albor[37], A. Gallas Torreira[37], J.A. Hernando Morata[37], A. Pazos Alvarez[37], E. Perez Trigo[37], M. Plo Casasus[37], P. Rodriguez Perez[37], J.J. Saborido Silva[37], B. Sanmartin Sedes[37], C. Santamarina Rios[37], M. Seco[37], P. Vazquez Regueiro[37], J. Visniakov[37]
[37] *Universidad de Santiago de Compostela, Santiago de Compostela, Spain*

J. Albrecht[38], F. Alessio[38], C. Barschel[38], T. Blake[38], E. Bonaccorsi[38], L. Brarda[38], J. Buytaert[38], M. Cattaneo[38], B. Chadaj[38], Ph. Charpentier[38], M. Chebbi[38], K. Ciba[38], M. Clemencic[38], J. Closier[38], P. Collins[38], B. Corajod[38], G. Corti[38], B. Couturier[38], C. D'Ambrosio[38], G. Decreuse[38], H. Dijkstra[38], R. Dumps[38], M. Ferro-Luzzi[38], R. Forty[38], C. Fournier[38], M. Frank[38], C. Frei[38], C. Gaspar[38], M. Gersabeck[38], V.V. Gligorov[38], L.A. Granado Cardoso[38], T. Gys[38], C. Haen[38], E. van Herwijnen[38], R. Jacobsson[38], O. Jamet[38], B. Jost[38], M. Karacson[38], R. Kristic[38], D. Lacarrere[38], E. Lanciotti[38], C. Langenbruch[38], R. Lindner[38], G. Liu[38], D. Martinez Santos[38], R. Matev[38], N. Neufeld[38], J. Panman[38], M. Pepe Altarelli[38], D. Piedigrossi[38], N. Rauschmayr[38], S. Roiser[38], L. Roy[38], T. Ruf[38], H. Schindler[38], B. Schmidt[38], T. Schneider[38], A. Schopper[38], R. Schwemmer[38], F. Stagni[38], V.K. Subbiah[38], F. Teubert[38], E. Thomas[38], D. Tonelli[38], M. Ubeda Garcia[38], O. Ullaland[38], M. Vesterinen[38], J. Wicht[38], W. Witzeling[38], K. Wyllie[38], A. Zvyagin[38]
[38] *European Organization for Nuclear Research (CERN), Geneva, Switzerland*

Y. Amhis[39], A. Bay[39], F. Bernard[39], F. Blanc[39], J. Bressieux[39], G.A. Cowan[39], H. Degaudenzi[39,38], F. Dupertuis[39], V. Fave[39], R. Frei[39], N. Gauvin[39], G. Haefeli[39], P. Jaton[39], A. Keune[39], M. Knecht[39], V.N. La Thi[39], N. Lopez-March[39], J. Luisier[39], R. Märki[39], B. Muster[39], T. Nakada[39], A.D. Nguyen[39], C. Nguyen-Mau[39,p], J. Prisciandaro[39], B. Rakotomiaramanana[39], J. Rouvinet[39], O. Schneider[39], P. Szczypka[39], S. Tourneur[39], M.T. Tran[39], G. Veneziano[39]
[39] *Ecole Polytechnique Fédérale de Lausanne (EPFL), Lausanne, Switzerland*

J. Anderson[40], R. Bernet[40], A. Büchler-Germann[40], A. Bursche[40], N. Chiapolini[40], M. De Cian[40], Ch. Elsasser[40], K. Müller[40], J. Palacios[40], C. Salzmann[40], S. Saornil Gamarra[40], N. Serra[40], O. Steinkamp[40], U. Straumann[40], M. Tobin[40], A. Vollhardt[40]
[40] *Physik-Institut, Universität Zürich, Zürich, Switzerland*

R. Aaij[41], S. Ali[41], H. Band[41], Th. Bauer[41], M. van Beuzekom[41], V. van Beveren[41], H. Boer Rookhuizen[41], L. Ceelie[41], V. Coco[41], P.N.Y. David[41], K. De Bruyn[41], P. De Groen[41], D. van Eijk[41], C. Farinelli[41], V. Gromov[41], B. van der Heijden[41], V. Heijne[41], W. Hulsbergen[41], E. Jans[41], F. Jansen[41], L. Jansen[41], P. Jansweijer[41], R. Kluit[41], P. Koppenburg[41], A. Kozlinskiy[41], J. van Leerdam[41], M. Martinelli[41], M. Merk[41], I. Mous[41],

B. Munneke[41], S. Oggero[41], M. van Overbeek[41], A. Pellegrino[41], O. van Petten[41], E. Roeland[41], K. de Roo[41], A. Schimmel[41], H. Schuijlenburg[41], T. Sluijk[41], B. Storaci[41], P. Tsopelas[41], N. Tuning[41], W. Vink[41], P. Wenerke[41], L. Wiggers[41], F. Zappon[41], A. Zwart[41]
[41] *Nikhef National Institute for Subatomic Physics, Amsterdam, The Netherlands*

J. van den Brand[42], F. Dettori[42], T. Ketel[42], R.F. Koopman[42], J. Kos[42], R.W. Lambert[42], F. Mul[42], G. Raven[42], M. Schiller[42], S. Tolk[42]
[42] *Nikhef National Institute for Subatomic Physics and VU University Amsterdam, Amsterdam, The Netherlands*

A. Dovbnya[43], S. Kandybei[43], I. Raniuk[43], I. Shapoval[43,38], O. Shevchenko[43]
[43] *NSC Kharkiv Institute of Physics and Technology (NSC KIPT), Kharkiv, Ukraine*

V. Iakovenko[44], Y. Nikolaiko[44], O. Okhrimenko[44], M. Pugatch[44], V. Pugatch[44]
[44] *Institute for Nuclear Research of the National Academy of Sciences (KINR), Kyiv, Ukraine*

P.J.W. Faulkner[45], I.R. Kenyon[45], C. Lazzeroni[45], J. McCarthy[45], M.W. Slater[45], N.K. Watson[45]
[45] *University of Birmingham, Birmingham, United Kingdom*

M. Adinolfi[46], J. Benton[46], N.H. Brook[46], A. Cook[46], M. Coombes[46], T. Hampson[46], S.T. Harnew[46], P. Naik[46], J.H. Rademacker[46], A. Solomin[46], D. Souza[46], J.J. Velthuis[46], D. Voong[46]
[46] *H.H. Wills Physics Laboratory, University of Bristol, Bristol, United Kingdom*

W. Barter[47], M.-O. Bettler[47], H.V. Cliff[47], J. Garra Tico[47], V. Gibson[47], S. Gregson[47], S.C. Haines[47], C.R. Jones[47], S. Sigurdsson[47], D.R. Ward[47], S.A. Wotton[47], S. Wright[47]
[47] *Cavendish Laboratory, University of Cambridge, Cambridge, United Kingdom*

J.J. Back[48], D. Craik[48], D. Dossett[48], T. Gershon[48,38], M. Kreps[48], T. Latham[48], T. Pilař[48], A. Poluektov[48,34], M.M. Reid[48], R. Silva Coutinho[48], M. Whitehead[48], M.P. Williams[48,49]
[48] *Department of Physics, University of Warwick, Coventry, United Kingdom*

S. Easo[49], R. Nandakumar[49], A. Papanestis[49], G.N. Patrick[49], S. Ricciardi[49], F.F. Wilson[49]
[49] *STFC Rutherford Appleton Laboratory, Didcot, United Kingdom*

S. Benson[50], P.E.L. Clarke[50], R. Currie[50], S. Eisenhardt[50], C. Fitzpatrick[50], D. Lambert[50], H. Luo[50], H. Mejia[50], F. Muheim[50], M. Needham[50], S. Playfer[50], A. Sparkes[50], Y. Xie[50]
[50] *School of Physics and Astronomy, University of Edinburgh, Edinburgh, United Kingdom*

M. Alexander[51], J. Beddow[51], S. Borghi[51,54], L. Eklund[51], D. Hynds[51], S. Ogilvy[51], M. Pappagallo[51], E. Rodrigues[51,54], P. Sail[51], F.J.P. Soler[51], P. Spradlin[51]
[51] *School of Physics and Astronomy, University of Glasgow, Glasgow, United Kingdom*

T.J.V. Bowcock[52], H. Brown[52], G. Casse[52], S. Donleavy[52], K. Hennessy[52], E. Hicks[52], T. Huse[52], D. Hutchcroft[52], M. Liles[52], G.D. Patel[52], K. Rinnert[52], T. Shears[52], N.A. Smith[52]
[52] *Oliver Lodge Laboratory, University of Liverpool, Liverpool, United Kingdom*

L. Carson[53], G. Ciezarek[53], S. Cunliffe[53], U. Egede[53], A. Golutvin[53,31,38], S. Hall[53], P. Owen[53],

C.J. Parkinson[53], M. Patel[53], K. Petridis[53], A. Richards[53], T. Savidge[53], I. Sepp[53], A. Shires[53], D. Websdale[53], M. Williams[53]
[53] *Imperial College London, London, United Kingdom*

R.B. Appleby[54], R.J. Barlow[54], T. Bird[54], P.M. Bjørnstad[54], D. Brett[54], J. Harrison[54], G. Lafferty[54], G. McGregor[54], D. Moran[54], C. Parkes[54], M. Smith[54], A.D. Webber[54]
[54] *School of Physics and Astronomy, University of Manchester, Manchester, United Kingdom*

M. Brock[55], M. Charles[55], N. Harnew[55], J.J. John[55], M. John[55], S. Malde[55], A. Nomerotski[55,38], A. Powell[55], C. Thomas[55], S. Topp-Joergensen[55], G. Wilkinson[55]
[55] *Department of Physics, University of Oxford, Oxford, United Kingdom*

B. Meadows[56], M.D. Sokoloff[56]
[56] *University of Cincinnati, Cincinnati, OH, United States*

M. Artuso[57,38], S. Blusk[57], A. Borgia[57], T. Britton[57], J. Garofoli[57], B. Gui[57], C. Hadjivasiliou[57], R. Mountain[57], B.K. Pal[57], A. Phan[57], W. Qian[57], T. Skwarnicki[57], S. Stone[57,38], J. Wang[57], Z. Xing[57], L. Zhang[57].
[57] *Syracuse University, Syracuse, NY, United States*

[a] *P.N. Lebedev Physical Institute, Russian Academy of Science (LPI RAS), Moscow, Russia*
[b] *Università di Bari, Bari, Italy*
[c] *Università di Bologna, Bologna, Italy*
[d] *Università di Cagliari, Cagliari, Italy*
[e] *Università di Ferrara, Ferrara, Italy*
[f] *Università di Firenze, Firenze, Italy*
[g] *Università di Urbino, Urbino, Italy*
[h] *Università di Modena e Reggio Emilia, Modena, Italy*
[i] *Università di Genova, Genova, Italy*
[j] *Università di Milano Bicocca, Milano, Italy*
[k] *Università di Roma Tor Vergata, Roma, Italy*
[l] *Università di Roma La Sapienza, Roma, Italy*
[m] *Università della Basilicata, Potenza, Italy*
[n] *LIFAELS, La Salle, Universitat Ramon Llull, Barcelona, Spain*
[o] *Port d'Informació Científica (PIC), Barcelona, Spain*
[p] *Hanoi University of Science, Hanoi, Viet Nam*

Contents

1 Introduction

With the Letter of Intent (LoI) for the LHCb Upgrade [1], submitted in March 2011, the LHCb Collaboration declared its interest in upgrading the detector to 40 MHz readout with a very flexible software-based trigger. This will allow the data rate to be increased substantially, as well as the trigger efficiency, leading to improvements in annual signal yields compared to those obtained by LHCb in 2011 by a factor of around ten for muonic B decays and twenty or more for heavy-flavour decays to hadronic final states. In addition to the significant increase in sensitivity for flavour physics, the experiment will be capable of triggering on other interesting signatures, such as long-lived particles, and thus act as a general purpose detector in the forward region.

Following encouragement by the LHCC to proceed to the detector Technical Design Reports (TDRs), it had been decided to first present this Framework TDR that provides information in particular about the schedule, cost and participating institutes. Based on the detailed studies presented in the LoI, this document gives an update on the expected physics performance, on the requirements to the detector and on the sub-systems R&D. A detailed discussion is then given of the schedule and cost of the different detector components, as well as the expression of interests from the collaborating institutes.

Since the sub-systems are in a period of R&D there are still a number of options open concerning the technologies, that are described here. Following the completion of the R&D phase, the remaining choices of baseline technology will be made in time for the sub-system TDRs, which will follow on a timescale of the next year or so. The overall schedule sees installation of the upgraded experiment in the second long shutdown of the LHC in 2018, to be ready for data taking in 2019.

1.1 Physics motivation

The detailed physics motivation for the LHCb upgrade is described in the Letter of Intent [1]. The LoI was, however, written when only about $35\,\text{pb}^{-1}$ of data had been recorded, accumulated from $\sqrt{s} = 7\,\text{TeV}$ pp collisions in 2010. During 2011 both the LHC machine and the LHCb detector performed superbly, allowing LHCb to accumulate $1.0\,\text{fb}^{-1}$ of $\sqrt{s} = 7\,\text{TeV}$ pp collisions that is available for physics analysis. Indeed, the results of many analyses based on some or all of this data set have already been submitted for publication. The results to date cover topics in the core flavour physics programme of LHCb in rare decays such as $B^0_s \to \mu^+\mu^-$ [2] and $B^0 \to K^{*0}\mu^+\mu^-$ [3] and in studies of CP violation, such as the measurement of the weak phase in B^0_s oscillations [4] and the first evidence for matter-antimatter asymmetries in both the charm sector [5] and in B^0_s decays [6]. It is therefore worthwhile to update the estimated performance that can be achieved by the upgraded detector in the light of these new results.

In addition, LHCb has continued to seek possibilities to enhance its physics reach by considering new analyses. To this end the collaboration organised two workshops, in Nov. 2011 and Apr. 2012, to discuss with invited theorists both the implications of its latest results and the prospects for new and improved measurements. These meetings

focussed mainly on the flavour physics aspects of the LHCb physics programme: they were organised with sessions on rare decays, *CP* violation in the B sector, and charm mixing and *CP* violation, with additional dedicated talks on the interplay of flavour physics and measurements from ATLAS and CMS. Nonetheless, it remains the case that the physics programme of the upgraded LHCb experiment extends beyond flavour physics. Indeed, the impact of LHCb measurements involving (for example) electroweak gauge bosons [7] has also been widely discussed both at dedicated workshops and in meetings on the implications of LHC results (ATLAS, CMS and LHCb) on TeV scale physics. A full report is being prepared on the outcome of the LHCb workshops with theorists, and the updated sensitivity studies for the upgrade [8], also in view of the preparation for the European Strategy for Particle Physics. Here only a brief summary is given.

To be conservative, the sensitivity studies reported in this document all assume detector performance as achieved during 2011 data taking. The exception is for the trigger efficiency, where channels selected by hadron, photon or electron hardware triggers are expected to have their efficiencies doubled (channels selected by muon triggers are expected to have marginal gains, that have not been included in the extrapolations). In reality the gain in trigger efficiency will vary channel by channel, and is expected to be significantly larger than the nominal factor of 2 for some charm decays, for example. More detailed studies of these effects, and of the impact of the new detector technologies to be used in the upgrade, are planned to be performed for the sub-system TDRs.

Several other assumptions are made for the upgrade:

- LHC collisions will be at $\sqrt{s} = 14\,\text{TeV}$, with heavy flavour production cross-sections scaling linearly with $\sqrt{s}$;
- the instantaneous luminosity in LHCb will be $\mathcal{L}_{\text{inst}} = 10^{33}\,\text{cm}^{-2}\,\text{s}^{-1}$: this will be achieved with 25 ns separation between bunches and an average number of visible interactions per crossing $\mu = 2$;
- the external crossing angle of the beams will be in the vertical plane (as already implemented for 2012 data taking), providing opposite beam crossing angles of equal amplitude for field-up and field-down polarities;
- LHCb will change the polarity of its dipole magnet with similar frequency as in 2011/12 data taking, to equalise approximately the amount of data taken with each polarity for better control of potential systematic biases;
- the annual integrated luminosity will be $\mathcal{L}_{\text{int}} = \mathcal{L}_{\text{inst}} \times t_{\text{LHC}} = 10^{33}\,\text{cm}^{-2}\,\text{s}^{-1} \times 5 \times 10^{6}\,\text{s} = 5\,\text{fb}^{-1}$ (where the expected LHC annual operational time t_{LHC} is consistent with current experience);
- the upgraded experiment will collect a total sample of $50\,\text{fb}^{-1}$.

The sensitivity to various flavour observables is summarised in Table 1. This is an updated version of a similar summary that appears as Table 2.1 in the LoI [1]. The

Type	Observable	Current precision	LHCb 2018	**Upgrade** ($50\,\text{fb}^{-1}$)	Theory uncertainty
B_s^0 mixing	$2\beta_s$ $(B_s^0 \to J/\psi\,\phi)$	0.10 [9]	0.025	0.008	~ 0.003
	$2\beta_s$ $(B_s^0 \to J/\psi\,f_0(980))$	0.17 [10]	0.045	0.014	~ 0.01
	$A_{\text{fs}}(B_s^0)$	6.4×10^{-3} [18]	0.6×10^{-3}	0.2×10^{-3}	0.03×10^{-3}
Gluonic penguin	$2\beta_s^{\text{eff}}(B_s^0 \to \phi\phi)$	–	0.17	0.03	0.02
	$2\beta_s^{\text{eff}}(B_s^0 \to K^{*0}\bar{K}^{*0})$	–	0.13	0.02	< 0.02
	$2\beta^{\text{eff}}(B^0 \to \phi K_S^0)$	0.17 [18]	0.30	0.05	0.02
Right-handed currents	$2\beta_s^{\text{eff}}(B_s^0 \to \phi\gamma)$	–	0.09	0.02	< 0.01
	$\tau^{\text{eff}}(B_s^0 \to \phi\gamma)/\tau_{B_s^0}$	–	5 %	1 %	0.2 %
Electroweak penguin	$S_3(B^0 \to K^{*0}\mu^+\mu^-; 1 < q^2 < 6\,\text{GeV}^2/c^4)$	0.08 [14]	0.025	0.008	0.02
	$s_0\,A_{\text{FB}}(B^0 \to K^{*0}\mu^+\mu^-)$	25 % [14]	6 %	2 %	7 %
	$A_{\text{I}}(K\mu^+\mu^-; 1 < q^2 < 6\,\text{GeV}^2/c^4)$	0.25 [15]	0.08	0.025	~ 0.02
	$\mathcal{B}(B^+ \to \pi^+\mu^+\mu^-)/\mathcal{B}(B^+ \to K^+\mu^+\mu^-)$	25 % [16]	8 %	2.5 %	~ 10 %
Higgs penguin	$\mathcal{B}(B_s^0 \to \mu^+\mu^-)$	1.5×10^{-9} [2]	0.5×10^{-9}	0.15×10^{-9}	0.3×10^{-9}
	$\mathcal{B}(B^0 \to \mu^+\mu^-)/\mathcal{B}(B_s^0 \to \mu^+\mu^-)$	–	~ 100 %	~ 35 %	~ 5 %
Unitarity triangle angles	γ $(B \to D^{(*)}K^{(*)})$	~ 10–12° [19, 20]	4°	0.9°	negligible
	γ $(B_s^0 \to D_s K)$	–	11°	2.0°	negligible
	β $(B^0 \to J/\psi\,K_S^0)$	0.8° [18]	0.6°	0.2°	negligible
Charm *CP* violation	A_Γ	2.3×10^{-3} [18]	0.40×10^{-3}	0.07×10^{-3}	–
	ΔA_{CP}	2.1×10^{-3} [5]	0.65×10^{-3}	0.12×10^{-3}	–

Table 1: Statistical sensitivities of the LHCb upgrade to key observables. For each observable the current sensitivity is compared to that which will be achieved by LHCb before the upgrade, and that which will be achieved with $50\,\text{fb}^{-1}$ by the upgraded experiment. Systematic uncertainties are expected to be non-negligible for the most precisely measured quantities.

measurements considered include *CP*-violating observables, rare decays and fundamental parameters of the CKM Unitarity Triangle. The current precision, either from LHCb measurements or averaging groups [18, 19, 20] is given and compared to the estimated sensitivity with the upgrade. As an intermediate step, the estimated precision that can be achieved prior to the upgrade is also given for each observable. For this, a total integrated luminosity of 1.0 $(1.5, 4.0)$ fb^{-1} at pp centre-of-mass collision energy $\sqrt{s} = 7$ $(8, 13)$ TeV recorded in 2011 (2012, 2015–17) is assumed. Another assumption is that the current efficiency of the muon hardware trigger can be maintained at higher $\sqrt{s}$, but that higher thresholds will be necessary for other triggers, reducing the efficiency for the relevant channels by a factor of 2 at $\sqrt{s} = 13$ TeV.

The extrapolations assume the central values of the current measurements, or the Standard Model where no measurement is available. While the sensitivities given include statistical uncertainties only, preliminary studies of systematic effects suggest that these will not affect the conclusions significantly, except in the most precise measurements, such as those of $A_{\rm fs}(B^0_s)$, A_Γ and ΔA_{CP}. Branching fraction measurements of B^0_s mesons require knowledge of the ratio of fragmentation fractions f_s/f_d for normalisation [21]. The uncertainty on this quantity is limited by knowledge of the branching fraction of $D^+_s \to K^+K^-\pi^+$, and improved measurements of this quantity will be necessary to avoid a limiting uncertainty on, for example, $\mathcal{B}(B^0_s \to \mu^+\mu^-)$. The determination of $2\beta_s$ from $B^0_s \to J/\psi\,\phi$ provides an example of how systematic uncertainties can be controlled for measurements at the LHCb upgrade. In the most recent measurement [9], the largest source of systematic uncertainty arises due to the constraint of no direct *CP* violation that is imposed in the fit. With larger statistics, this constraint can be removed, eliminating this source of uncertainty. Other sources, such as the background description and angular acceptance, are already at the 0.01 rad level, and can be reduced with more detailed studies.

In the Standard Model (SM), the parameters of *CP* violation in B^0_s mixing are highly constrained to be close to zero by global fits to the CKM matrix. LHCb has measured the mixing phase $2\beta_s = -\phi_s$ in both $J/\psi\,\phi$ and $J/\psi\; f_0(980)$ final states, with results that are consistent with the SM within the uncertainties [9, 10]. However, tensions in the global CKM fits (see, for example, Ref. [11]) suggest that deviations may be present at the level of a few degrees (~ 0.04 rad, in the units of Table 1), motivating much more precise measurements. A complementary measurement, $A_{\rm fs}$, can be made using semileptonic decays. This analysis requires excellent control of systematic uncertainties to be sensitive to small deviations from the SM prediction of $\mathcal{O}(10^{-4})$.

Decays dominated by $b \to s$ loop (penguin) transitions provide additional sensitivity to contributions beyond the SM. The B^0_s decays to $\phi\phi$ and $K^{*0}\overline{K}^{*0}$ final states, both already observed at LHCb [12, 13], are particularly interesting since these effects could appear in both time-dependent and angular distributions. Another important measurement is that of the time-dependent decay distribution in $B^0_s \to \phi\gamma$ decays. Determination of the effective *CP*-violation and lifetime parameters provides the most promising way to study the polarisation of the emitted photon, and is therefore uniquely sensitive to models that predict new right-handed currents.

Rare decays involving dimuon pairs constitute a significant part of the flavour physics programme of the LHCb experiment, and this will remain the case in the upgrade. As statistics increase, a larger set of angular observables in $B^0 \to K^{*0}\mu^+\mu^-$ decays can be measured. The first measurement of the zero-crossing point (s_0) of the forward-backward asymmetry in this decay has recently been presented by LHCb [14], demonstrating the potential for the upgrade to fully explore the phase space for contributions beyond the SM. Another important observable with low theoretical uncertainty is the transverse polarisation asymmetry, which is probed by the parameter S_3.

LHCb has also recently published the world's most precise measurements of isospin asymmetries in $b \to s\mu^+\mu^-$ decays [15]. These have generated significant interest in the theory community, and this sector will be further explored as more data are accumulated. Similarly, the first observation of $B^+ \to \pi^+\mu^+\mu^-$ [16] shows the potential for a measurement of $|V_{td}/V_{ts}|$ in loop-mediated transitions. Note that some values quoted in Table 1 are integrated over the dimuon invariant mass range $1 < q^2 < 6\,\mathrm{GeV}^2/c^4$ to give a representative estimate of the sensitivity – however the full differential distribution will be studied.

The rare decay $B_s^0 \to \mu^+\mu^-$ is a golden channel to search for effects beyond the Standard Model. Although the latest measurement from LHCb [2] rules out new contributions of comparable size to that from the SM, much more precise measurements are well motivated since the theoretical prediction for the branching fraction has low uncertainty and the true value may be smaller than the SM expectation. With the $50\,\mathrm{fb}^{-1}$ data set it will also be possible to measure the rate of the B^0 decay to two muons down to the SM prediction: the ratio of B^0 to B_s^0 branching fractions is given by $|V_{td}/V_{ts}|^2$ in the SM and any extension with minimal flavour violation, making this a crucial channel to diagnose the origin of any non-SM contributions.

The measurement of the angle γ of the Unitarity Triangle from $B \to DK$ decays is a SM benchmark. The first results from LHCb [17] already make a significant impact on the global averages – however, measurements at the degree-level of sensitivity are necessary to match the precision in lattice QCD. Similarly, improved measurements of the angle β will further constrain the global fits, and may reveal contributions beyond the SM if the "tensions" that are present in the current data persist.

In the charm sector, the evidence for *CP* violation from LHCb [5] has prompted a great deal of theoretical interest, which has highlighted several other observables that should be measured. Although hadronic uncertainties cloud the interpretation of the current measurement, when additional observables are measured it will be possible to constrain these effects, and hence to determine if the origin of the asymmetry is from physics beyond the SM. It is particularly important to be able to distinguish *CP*-violation effects from charm mixing and those from decay.

Although other experiments will study flavour-physics observables in a similar timeframe to the LHCb upgrade, the sample sizes in most exclusive B and D final states will be far larger than those that will be collected elsewhere, for example at the upgraded e^+e^- B factories. The LHCb upgrade will have no serious competition in its study of B_s^0 decays and *CP* violation. Similarly the yields in charmed-particle decays to final states

consisting of only charged tracks cannot be matched by any other experiment.

It must be emphasised that in addition to the physics summarised in Table 1, the upgraded experiment will have exciting opportunities to perform studies that will shed light on the lepton sector, and in topics beyond flavour physics. LHCb will be best-placed of all the LHC experiments to make an improved determination of the effective electroweak mixing angle, and to combat the systematic uncertainties from parton distribution functions that may limit the ATLAS and CMS efforts to measure the mass of the W boson. LHCb will have high sensitivity in the search for new particles with long lifetimes, and will be able to make QCD studies which are complementary to those possible in the central region. First results on some of these topics have recently been reported [22, 23], and will help to develop further the physics studies for the sub-system TDRs.

1.2 Evolution of requirements and main technical options

Since submission of the Letter of Intent there has been some evolution of requirements to the upgraded detector and of the main technical options. In the LoI we considered operating the upgraded detector at a luminosity of $\mathcal{L} = 1 \times 10^{33}\text{cm}^{-2}\text{s}^{-1}$ with a fully flexible software trigger running at a readout rate of 40 MHz. This increases the annual signal yields by a factor of around ten for muonic B decays and twenty or more for heavy-flavour decays to hadronic final states, as compared to those obtained by LHCb in 2011.

For reasons of flexibility, and to allow for possible evolutions of the trigger, we have decided to design those detectors that need replacement for the 40 MHz upgrade such that they can sustain a luminosity of $\mathcal{L} = 2 \times 10^{33}\text{cm}^{-2}\text{s}^{-1}$. For the other detector components we are evaluating the effect of such a luminosity increase. As already discussed in the LoI, operating the detector at $\mathcal{L} = 2 \times 10^{33}\text{cm}^{-2}\text{s}^{-1}$ has in particular consequences for the area to be covered by the Inner Tracker in order to keep the occupancy in the Outer Tracker at a reasonable level. To account for this we are investigating two main tracker options, a large area silicon-strip Inner Tracker complemented by Outer Tracker straw tubes, or a Central Tracker made from scintillating fibres. The Central Tracker is an evolution of the scintillating-fibre Inner Tracker described in the LoI, extending the active area of scintillating fibres to the detector periphery. In parallel to the technical R&D we are also studying optimization of the overall tracker layout. This includes re-optimization of the position of the individual tracking stations as well as their acceptance coverage.

The other sub-detector for which alternative technology options exist is the Vertex Locator, where the choice is between strip and pixel sensors. For both options we are investigating whether the impact parameter resolution can be improved by moving the sensors closer to the beam as compared to the current detector.

In the following we describe the main evolution in R&D of the different technologies that are under consideration for the Tracker System, for the Particle Identification detectors, and for Data Processing. The Tracker sub-systems are the Vertex Locator (VELO) made from silicon strips or pixels, the Trigger Tracker (TT) and Inner Tracker (IT) made from silicon strips, the Central Tracker (CT) made from scintillating fibres, and the Outer

Tracker (OT) made from straw tubes. The Particle Identification detectors are the Ring Imaging Cerenkov (RICH) detectors, the electromagnetic (ECAL) and hadronic (HCAL) calorimeters, as well as the Muon system. The data processing is sub-divided into Trigger, Data Acquisition (DAQ) and Computing.

In the last chapter the individual sub-system schedules are presented, indicating the major milestones, together with a first cost estimate and the list of participating institutes.

1.3 Requirements to the LHC

Although the intended instantaneous luminosity for the upgrade of LHCb of up to $\mathcal{L} = 2 \times 10^{33}\text{cm}^{-2}\text{s}^{-1}$ is far below the LHC design luminosity, the envisaged instantaneous luminosity has implications for the operation of the LHC. This has been presented and discussed at the Chamonix 2012 workshop [24].

A bunch spacing of 25 ns is essential for the LHCb upgrade, to limit the pile-up of pp interactions at the increased luminosity. In order to maintain a luminosity of $\mathcal{L} = 2 \times 10^{33}\text{cm}^{-2}\text{s}^{-1}$ at LHCb throughout a fill of typically 8 hours length by luminosity leveling, the virtual luminosity at the beginning of the fill has to be about four times larger. The resulting value is close to the LHC design luminosity of $\mathcal{L} = 1 \times 10^{34}\text{cm}^{-2}\text{s}^{-1}$. In order to protect the triplet quadrupole magnets and other machine elements from particles leaving the interaction point (IP) at such luminosities, the high luminosity insertions at IP1 and IP5 are equipped with a Target Absorber for Secondaries (TAS) and Neutral particles (TAN). The question whether a TAS and/or a TAN would also be needed at IP8 is currently addressed in discussions with the machine groups and detailed FLUKA simulations are planned.

Furthermore, in order to maintain a luminosity of $\mathcal{L} = 2 \times 10^{33}\text{cm}^{-2}\text{s}^{-1}$ at LHCb throughout a fill, beams would have to be focused in IP8 to a β^* of about 3.5 m. The option of an Achromatic-Telescopic Squeezing (ATS) scheme to get to β^* values as low as 0.1 m at the high luminosity IPs has a strong impact on the optics and the matching section of the neighboring LHC sectors, hence also on IP8. Studies are ongoing to develop possible ATS optics compatible with the LHCb upgrade requirement and first results are very encouraging [25].

Issues in relation to the expected radiation levels due to the higher luminosity are addressed as well. The relocation of some electronics equipment of the machine such as PLCs (programmable logic controllers) is foreseen already in the first long shutdown (LS1). More simulations are ongoing to determine whether other equipment needs to be mitigated for the proposed upgrade scenario.

Finally, as mentioned in Sec. 1.1, in order to control well the systematic uncertainties in the measurement of CP asymmetries with LHCb, it is of particular importance that equal amounts of data are taken with the two spectrometer polarities, and that the polarity of the LHCb dipole magnet is changed with a frequency similar to 2011/2012. For 25 ns bunch spacing, as required for the upgrade, this is only possible if the external crossing angle is in the vertical plane. As a consequence the effective crossing angle for both

magnet polarities will have the same absolute value and will be in a tilted plane. The implementation of the external vertical crossing has already been done successfully for the LHC physics run in 2012. However, due to the orientation of the beam screen in the inner triplet, an external vertical crossing angle already at injection has very little aperture and the change of the crossing plane is only done at the end of squeeze. In order to simplify this for the long-term future it is important that the beam screen in the inner triplet is rotated.

All these issues are addressed in discussion with the machine groups and by the recently formed HL-LHC Coordination group.

2 Evolution of sub-system R&D since the LoI

2.1 Tracking systems

In the LoI the role of the tracking detectors in LHCb and their performance in the current experiment were presented. The main challenges for the LHCb upgrade were described and a number of exploration paths have been outlined. Since the LoI, a few points have been reconsidered. The main changes are the following:

- The current LHCb Tracker stations are composed of an OT with straw tube detectors and an IT with silicon strip detectors to cover the high-occupancy area near the beam pipe. A new technology for the IT upgrade, based on scintillating fibres, was introduced in the LoI, with clear fibres carrying the signal photons from the inner region to the detectors situated outside the LHCb acceptance. In the mean time, a new scintillating-fibre layout has been proposed, with 2.5 m long fibres covering the whole central region of the Tracker stations, from the LHC beam plane all the way to the top and bottom of the LHCb acceptance. In this CT option, the IT and several OT modules are replaced by the new scintillating-fibre modules. The alternative solution, the IT option, is being explored in parallel and proposes to cover with silicon microstrip sensors an area larger than that covered by the current IT detector. The two options (CT and IT) are illustrated in Fig. 1.

- The decision has been taken that any change to the LHCb detector should be made such that the new implementation is compatible with operation at a leveled, i.e. constant, luminosity of 2×10^{33} cm^{-2}s^{-1}. The consequences for each Tracker subdetector are briefly discussed below.

- Investigations about a possible reduction of the inner foil radius of the VELO have been launched. The impact of such a change are outlined below in the VELO subsection.

A summary of the detector upgrade layout options for the VELO and Trackers is given in Table 2.

Subsystem	Technology options
VELO	microstrip silicon sensors pixel sensors
TT	microstrip silicon sensors
Tracker stations	OT straw tubes + CT scintillating fibres OT straw tubes (new short modules) + large area silicon IT

Table 2: Summary of detector layout options for the VELO and tracker upgrades.

In the following, the various design options of the tracking detectors and the simulation/reconstruction strategy to reach an optimal design choice are briefly reviewed with an emphasis on the evolution since the LoI.

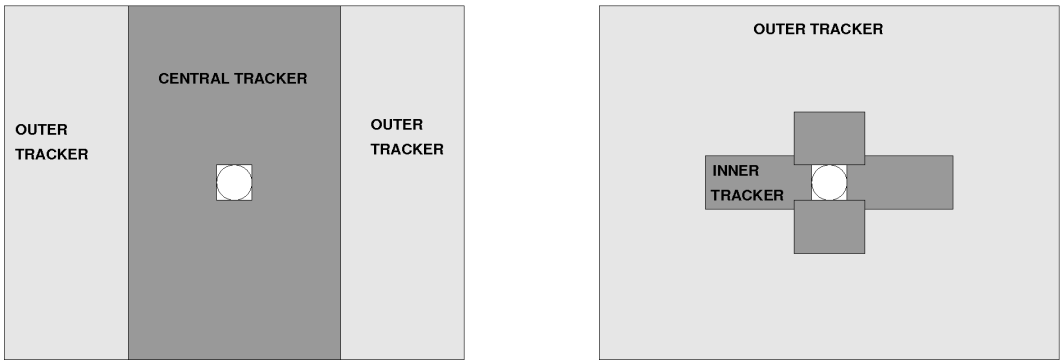

Figure 1: Schematic layouts of the two options being studied for the upgrade of the LHCb tracking stations (not to scale). Left: OT straw tubes (light grey area) with scintillating-fibre CT (dark grey area). Right: OT straw tubes (light grey area) with IT made of microstrip silicon sensors (dark grey area). The central hole is for the beam pipe.

2.1.1 Vertex Locator

The proposed geometry of the detector remains unchanged since the LoI, and a global summary of the important performance parameters at 2×10^{33} cm^{-2}s^{-1} are given in Table 3 for the pixel and strip options.

Concerning work for the pixel option, the design of the Timepix3 chip, the precursor to the Velopix ASIC (Application Specific Integrated Circuit), is progressing well, with a chip submission planned for Q3 2012. The design of the Velopix readout is nearing completion, using detailed simulations of high-luminosity data. Many possible super-pixel geometries have been simulated, with a 4×4 super-pixel architecture found to be optimal in terms of data compression and sharing of hardware. The output data format has been updated to a simplified version, which achieves the same compression performance as previously, but is optimised for the subsequent processing steps. At a luminosity of 2×10^{33} cm^{-2}s^{-1} less than 1% of hits are lost in the architecture, for the chips with the highest data rates. The hottest chips (of which there are two per half station) will see rates of approximately 500 MHz pixel hits and will output 12.2 Gbit/s. The total data rate for the pixel solution is approximately 2.8 Tbits/s.

The higher luminosity of the upgrade leads to increased occupancy for strips compared with the current implementation. For the prototype strip detector with 30 μm innermost pitch, occupancies of about 1.2% are expected for minimum bias events at 2×10^{33} cm^{-2}s^{-1}, with 1.8% for events containing a B decay within the acceptance. However, due to the variable pitch design, the data rates are spread approximately evenly amongst the ASICs, with an average of 1.4 Gbit/s, and a total data rate for the entire detector of 2.3 Tbit/s. The reduced number of bits per strip cluster is offset by the greater number of clusters (an R and a Phi cluster for each single pixel cluster). A design has been made for a strip detector with minimum pitch of 30 μm, which uses the second metal layer to group the readout channels from similar regions into the same ASIC. Delivery is expected in Q2 2012, and if the design proves successful a move to smaller minimum pitch can be

considered. A pitch of 25 μm should be readily achievable, however the challenge will be to map the larger number of readout channels to the ASICs.

	Strips, 128 (256) channel ASIC	Pixels
# ASICs / half station	40 (20)	12
# half stations	42	52
# ASICs total	1680 (840)	624
# sensors total	84	104
Silicon sensor area (m^2)	0.187	0.087
# channels total	215k	41M
Cluster size	1.6 (1.6)	2.2
# clusters / half station / 25 ns	52.6 (52.6)	25.8
# pixel (strip) hit / half station / 25 ns	84.2 (84.2)	56.8
# bits / cluster	42.4 (34.4)	52.3
# bits / pixel (strip) hit	26.5 (21.5)	23.8
Hottest chip output rate	1.4 Gbit/s (2.2)	12.2 Gbit/s
Coolest chip output rate	1.4 Gbit/s (2.2)	1.5 Gbit/s
Data rate / half station	56 Gbit/s (45)	54.3 Gbit/s
Total data rate	2352 Gbit/s (1880)	2823 Gbit/s

Table 3: Summary of VELO design parameters.

Based on experience with the current LHCb detector and LHC beams, it appears that several parameters which originally limited the minimum distance of approach of the RF foil material can be reconsidered. The beam positions are stable during physics data taking, the VELO positioning is precise and reliable, and the detector halves are accurately adjusted around the luminous region at each and every fill. Preliminary considerations indicate that the current inner foil radius of 5.5 mm could be reduced to less than 4 mm, perhaps as low as 3 mm. This, potentially, would allow the inner radius of the sensitive area of the silicon sensor to be reduced from the current 8.2 mm to 7 mm, perhaps even 6 mm, which would have a major impact on the LHCb physics performance, owing to the improved impact parameter resolution. Effort is underway to assess all consequences and benefits of such a radius reduction. Limitations from the beam size, beam excursions and foil manufacturing tolerances, effects of the beam image currents in the RF foil, are now being studied and will be discussed with LHC machine experts to define a new limit for the inner foil radius. Restrictions arising from the larger fluence and data rates in the inner detector area, and of the achievable silicon segmentation, are currently being investigated. A decision on the inner foil radius must be taken soon, by Q4 2012, as it has consequences for several aspects of the VELO detector design.

Work has progressed on the RF foil, which is very complex to manufacture. It is a critical item for the performance of the upgraded detector, as it dominates the material up to the second measured point. A new manufacturing technique is under development that is particularly important for the L-shaped foil for the pixel option, but also of advantage

for the strip option. The shape is milled out of the inside of a solid aluminium alloy block, which is then filled, and the opposite side is then milled to the desired thickness. The first round of prototyping has proven to be very successful, with a double demonstrator box with thickness close to target and leak rates better than 10^{-6} mbarℓ/s being produced. A new large plan 5-axis CNC milling machine has been purchased and first tests are currently underway. Work has also progressed on the simulation front, in order to best optimize the exact shape and depth of the corrugations (see Sec. 2.1.5 below). This work is showing promising first results, and will be used together with the flexibility of the milling approach in terms of minimum radii and foil shapes to optimize the design.

The module construction and the readout chain have seen significant progress. The flex cable links carrying the analogue signals to the vacuum tank feedthroughs have been prototyped and constructed in Dupont Pyralux AP-plus, a new material specifically developed for high speed applications which exhibits electrical characteristics necessary for the upgrade application, and in addition is straightforward to manufacture, with techniques similar to the treatment of kapton. Testbench systems with FPGA development boards have been set up and initial results are very encouraging, showing that the length and flexibility needed for the mechanical performance in the moving VELO halves can be achieved. Three main techniques are under active investigation for the cooling of the module itself. The first is a demountable solution with invar tubes mounted in a TPG-CF sandwich cooling block, in conjunction with a through-hole copper plated TPG substrate. An alternative approach is silicon microchannel cooling, whereby the cooling fluid runs below the ASICs, removing heat very efficiently and giving an ideal match in terms of thermal expansion coefficients, removing the need for the diamond substrate. Work is underway to produce prototypes to check the suitability of this method for the pressure and manifold designs suitable for CO_2 cooling, and first demonstrators are expected by Q3 2012. Planar pixel sensors have been produced by two manufacturers, and negotiations are continuing with further producers. These will be tested for performance and radiation hardness in 2012.

2.1.2 Trigger Tracker

The overall design concept has not changed since the LoI. The baseline option remains a 4-plane solution, with finer y segmentation and full coverage in the detector acceptance. A detailed model of this detector concept has been developed and will be introduced in the detector simulation framework soon. Variations of this design including finer segmentation in the direction perpendicular to the LHCb dipole field direction, and additional planes for more robust tracking, will be studied as well. The performance studies based on Monte-Carlo simulation with different designs are discussed further in Sec. 2.1.5.

The sensors in the innermost region are expected to be exposed to radiation levels of the order of 1×10^{14} $n_{\rm eq}\,{\rm cm}^{-2}$. At this fluence the RD50 collaboration has demonstrated that 300 μm thick n-in-p sensors achieve essentially full charge collection at 500 V [26]. On the other hand, the fluence is decreasing rapidly with the distance from the beam axis, and at a radius of about 20 cm from the beam axis p-in-n devices are perfectly adequate.

Thus, a combination of the two sensor technologies can be envisaged. At a luminosity of 2×10^{33} cm^{-2}s^{-1}, the track density in the sensors located near the beam pipe will be such that a strip length of a few cm should be considered. The current conceptual design proposes to use 9.8×9.8 cm^2 sensors segmented into 1, 2 or 4 sectors (depending on the location of the sensor) of 512 strips each and with a pitch of 183 μm (as in the current TT detector). Thus, those closest to the beam axis have four rows of 2.5 cm long strips, each with 4 front-end (FE) ASICs (16 per 4-sector sensor). The 2-sector sensors have two rows of 5 cm long strips (i.e. 8 ASICs per sensor). The 1-sector sensors are similar to the current TT sensors. It is being considered to mount the FE hybrids directly on the sensors, a concept inspired by the design for the silicon strip staves of the ATLAS upgrade tracker. Compared to the current TT design, this concept introduces the FE hybrid material in the region of highest track density and requires the implementation of an adequate cooling mechanism to remove the heat from the densely packed FE ASICs. However, this is balanced with the advantage of a much reduced input capacitance, hence a lower input noise, which may facilitate usage of significantly thinner sensors. The current TT sensors are 500 μm thick, while a thickness of 300 μm or less is being considered for the TT upgrade. Thinner sensors imply less material in the acceptance and reduced power dissipation from the product of leakage current and depletion voltage.

An important challenge in this system is the mechanical design, which includes the cooling strategy. A design is being studied which is based on a low-mass active cooling concept similar to the one developed for the CMS and ATLAS silicon tracker upgrades [27, 28] and already described in the LoI. A mock-up TT stave is being constructed in order to study and optimize the stave design. From these tests and from model calculations, the affordable sensor thickness and the cooling strategy will be defined, taking into account expected signal-over-noise ratio, needed spatial resolution, required temperature at maximum fluence and material distribution.

Specifications for the FE electronics consistent with the proposed sensor design have been developed and are used in the FE electronics design discussed in Sec. **??**. The main features that are important to the TT design are power minimization, as it is planned to mount the thinned electronics near the sensors to avoid cross talk problems related to long cables, and fast return to the baseline to avoid spillover hits. If these conditions are satisfied, binary readout is sufficient in data-acquisition mode, since charge interpolation between strips is not expected to bring much improvement for the strip pitch value under consideration.

2.1.3 Tracker stations

As already described in the LoI, current experience with the LHCb detector and preliminary Monte-Carlo simulation results show that the occupancy in the inner area (near the beam pipe) will become too large for the most central OT straw tube modules at the LHCb upgrade luminosity. A new design of the detectors in the central area is needed, along with a new definition of the inner (or central) and outer regions.

In the LoI, several exploratory solutions were exposed, such as replacement of the

silicon IT by thin scintillating fibres, replacement of the central OT straw modules by thick scintillating fibres, and replacement of the current silicon IT by a larger area silicon IT (with shorter OT straw modules).

Two solutions are currently being studied in parallel. A conceptual design of a large-area IT has been produced, while the scintillating-fibre design effort is now concentrating on a design in which thin-fibre modules replace the central OT modules and the IT.

Both solutions foresee the presence of straw-tube modules to cover the remaining detection area (with the IT solution requiring the additional production of shorter straw-tube modules). All straw-tube modules will be equipped with new FE and readout electronics compatible with 40 MHz data acquisition, as described in detail in the LoI.

The issue of radiation resistance of both the fibres and SiPM for their readout was already mentioned in the LoI and is being extensively studied. Important questions regarding the viability of this technology will be addressed this year (2012), so that the effort can be focussed on the optimization of the Tracker stations with a limited combination of detector technologies.

Silicon strip Inner Tracker

As presented in the LoI, the present IT detector has hardly any deterioration in tracking efficiency at 2×10^{33} cm^{-2}s^{-1} compared to the (current LHCb) nominal luminosity [1]. A new silicon strip IT, if sufficiently large, would give a sound solution in combination with shorter OT modules in the central region.

A substantial fraction of the hits in the OT originate from secondary particles generated in the beam-pipe support and IT detector, mainly from photon conversions. Hence, if redesigned, two considerations are of primary importance: (a) increase the transverse size of the IT detector to push out the inner limit of the OT edge and (b) improve the IT detector transparency to reduce further the OT occupancy in the innermost region. The choice of the minimum hole size is currently being investigated with a detailed LHCb upgrade simulation, which includes as one of the options a lighter silicon IT detector description (see Sec. 2.1.5).

The current LHCb IT detector has a "swiss cross"-like geometry with transverse dimensions width$\times$height $\approx 126 \times 22$ (41) cm^2 (the number in brackets designates the detector height in the central part, across the beam pipe). A maximum OT occupancy of 25% in the hottest straw could be achieved with an IT detector of dimensions $\approx 255 \times 42$ (63) cm^2, which would have approximately four times as many silicon sensors as in the present IT. The track fraction covered by the IT would increase from 33% to 54%.

Preliminary results on detector occupancy were obtained with the LHCb Monte-Carlo simulation package described in Chapter 11 of the LoI [1], in the so-called "minimal upgrade" configuration (lighter beam pipe support, IT/OT z positions swapped). Figure 2 shows the expected occupancy at $\mathcal{L} = 2 \times 10^{33}$ cm^{-2}s^{-1} for inclusive B events at $\sqrt{s} =$ 14 TeV. Three cases are compared:

(a) with the current LHCb IT detector ($\approx 126 \times 22$ (41) cm^2);

(b) with a larger IT coverage (2-sensor ladders, $\approx 255 \times 42$ (63) cm^2);

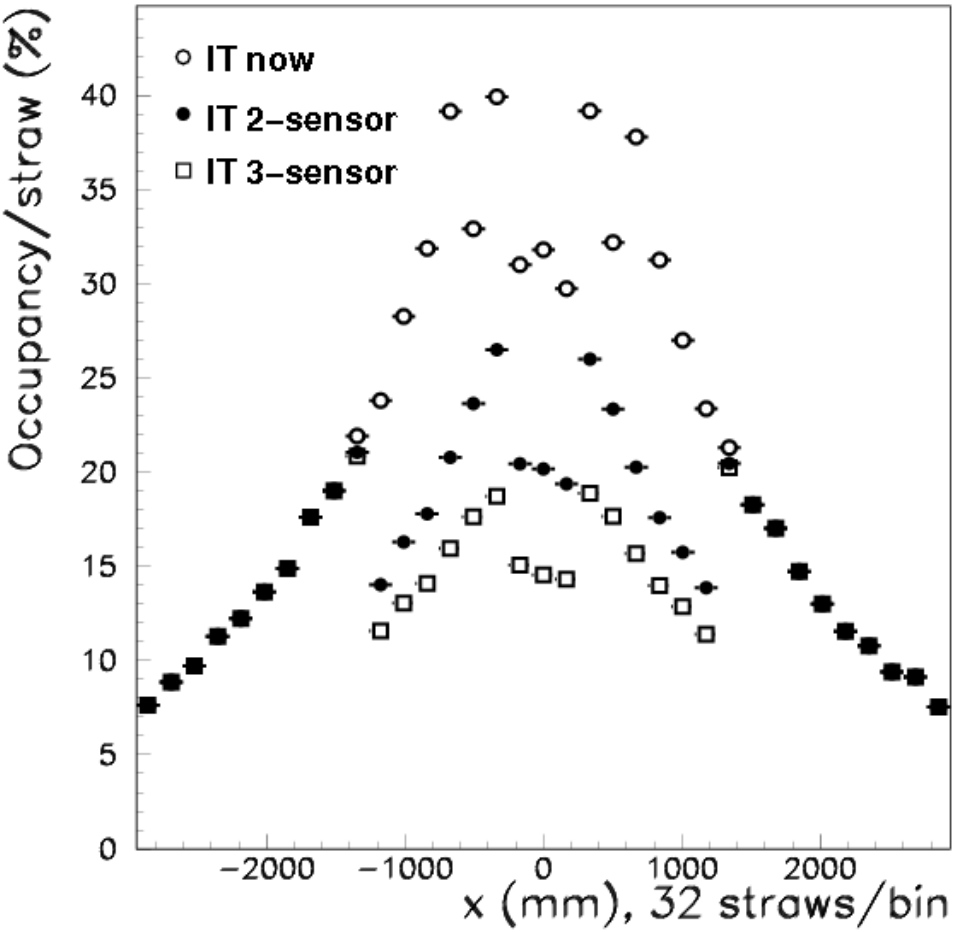

Figure 2: OT occupancy as a function of x for three different IT configurations in the "minimal upgrade" LHCb simulation (see text).

(c) with an even larger IT coverage (3-sensor ladders, $\approx 255 \times 63$ (84) cm^2).

Note that, in all three cases, the IT/OT material description was that of the current LHCb detector (no benefit from a lighter IT design). The OT hits falling inside the redefined inner hole were simply not counted as OT hits. The main conclusions are that an OT occupancy of 25% or less seems within reach with 2-sensor ladders (and a mass-optimized detector), while an OT occupancy of less than 20% could be achieved straightforwardly with 3-sensor ladders. What occupancy is acceptable in the hottest OT region will soon be determined with the LHCb upgrade simulation.

Three concepts are being studied to minimize the amount of material with respect to the current LHCb design:

1. Convective cooling: use of convective heat transfer for cooling, instead of bulk conduction, will drastically reduce the amount of material in the acceptance. Radiation aging simulations show that a silicon temperature between 0 and 10 °C will be suffi-

cient for an upgrade silicon IT. The conceptual design thermally isolates the silicon ladders from the FE electronics, which are the dominant heat source. The use of thin flex cables inspired by the ALICE design [29] is being studied. With a 10 cm flex cable a signal-over-noise ratio of more than 10 can easily be achieved. This approach would also push out the FE hybrid to regions of lower particle flux. Preliminary estimations show that cold gas circulation is largely sufficient to maintain the silicon at the desired temperature while efficiently evacuating the heat from the FE electronics. Thermal simulation studies are underway and an air-cooled mock-up is being manufactured in order to demonstrate the feasibility of this conceptual design and to explore its operational aspects.

2. Self-supporting ladders: the rigidity of the silicon sensors will be exploited to minimize additional supporting material, and silicon sensors will be made to overlap within a ladder. Sensor-to-sensor bump bonding is being investigated, though conventional wire bonding can also be applied.

3. Minimization of the number of IT layers: currently, 12 layers are used, while performance measures indicate that 10 layers may be sufficient. This is being studied with the detailed simulation described in Sec. 2.1.5.

Scintillating-fibre Central Tracker

Tracking downstream of the dipole magnet with scintillating-fibre modules in the central region is being considered. In this new configuration, the existing outermost straw tube modules, four on each side, are kept as in the current LHCb detector and their electronics upgraded to allow readout at 40 MHz. The central part (OT and IT) is replaced with scintillating fibre modules covering the full height of the detector. The upper and lower halves of the modules contain 2.5 m long scintillating fibres, separated with mirrors at the inner boundary and read out with Silicon Photomultipliers (SiPM) mounted outside the LHCb acceptance. With this configuration, passive material in the detector acceptance is minimized and exposure to radiation is reduced for the SiPMs and FE electronics.

One of the key R&D challenges will be to determine how the SiPM performance will evolve as a function of radiation dose and under what conditions these photon detectors will represent a viable solution for the LHCb CT. The radiation fluence at the SiPM location is expected to be of the order of 10^{12} $n_{\rm eq}\,{\rm cm}^{-2}$. Besides previously described irradiation studies with 65 MeV protons and with neutrons from a PuBe source [1], SiPM samples have been placed in the LHCb detector at the bottom of the tracking stations during the 2011 data taking period. Figure 3 shows the result of this SiPM irradiation study. The red triangles show, as a function of time, the leakage current of a sample SiPM that was mounted in 2011 at the position of the OT readout boxes and not shielded. The blue squares show the same for a sample SiPM in a similar location, but shielded with 100 mm of polyethylene containing 5% boron. This SiPM sample shows an increase in dark current that is approximately a factor two lower than for unprotected sensors at the same location. Adding 1 mm of Pb shielding (and then 1 mm of Cd) between the SiPM

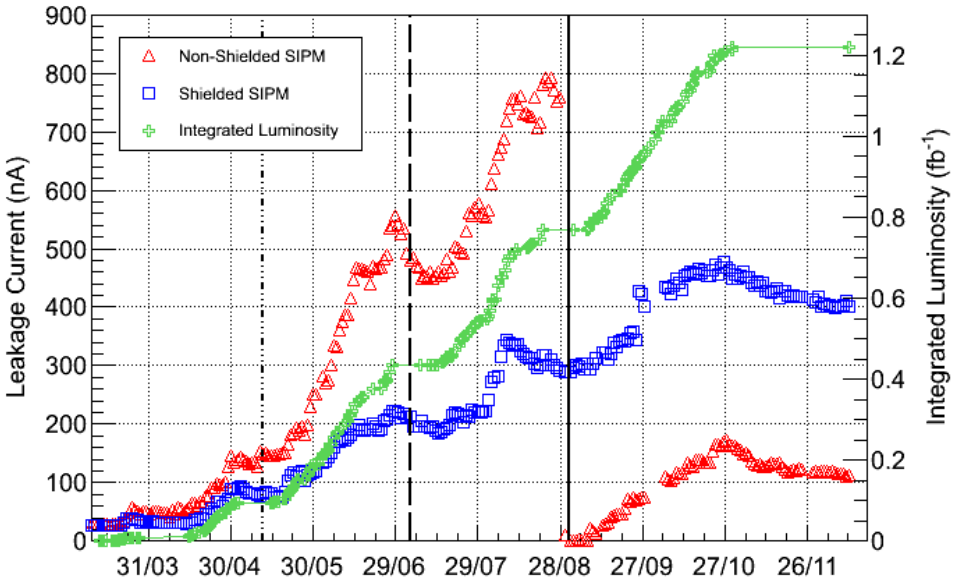

Figure 3: Result of an irradiation study of SiPM. The red triangles show, as a function of time, the leakage current of a sample SiPM that was mounted at the position of the OT readout boxes and not shielded. The continuous vertical line indicates the date when the SiPM was replaced with another one of different pixel size. The blue squares show the leakage current of a sample SiPM in a similar location, but shielded with polyethylene. The dot-dashed (dashed) vertical line indicates the date when the shielding was increased by adding 1 mm of Pb (1 mm of Cd) between the SiPM and the polyethylene. The green crosses show the integrated luminosity at IP8 in 2011 (scale on the right axis).

and the polyethylene had little impact on the evolution of the leakage current. The effects of radiation damage can also be reduced by operating the SiPMs at low temperature. The dark current is predicted to be reduced by a factor 2 for about every 8 °C temperature step. The option to cool the SiPM is being studied, with a temperature as low as −25 °C being considered. This R&D effort will determine whether a combination of neutron shielding and active cooling will allow the SiPM lifetime to be extended to the required level. The signal deterioration due to radiation damage in the fibres was already mentioned in the LoI and will now be measured on irradiated 2.5 m modules.

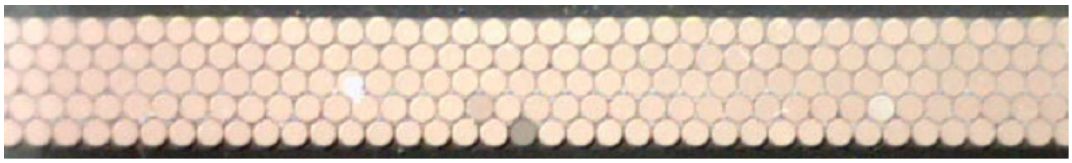

Figure 4: Cross section photograph of a recently built 2.5 m long scintillating-fibre module.

The techniques for the production of fibre matrices are still under development for

both methods presented in the LoI, namely winding fibres on a cylindrical surface of radius larger than 40 cm or on a long cuboid. Dummy fibre matrices have been produced with both methods. Recently, a 2.5 m long sample module has been fabricated on the cylindrical barrel with scintillating fibres of 0.25 mm diameter. The sample contained five layers of about 100 fibres each. Figure 4 shows a photograph of the cross section of this 2.5 m long module. The distance between the centres of adjacent fibres was measured. Figure 5 shows that the fibres are positioned with an accuracy of 6 μm (RMS) relative to each other. Such prototype modules will be characterized with SiPM readout and test beam particles in 2012.

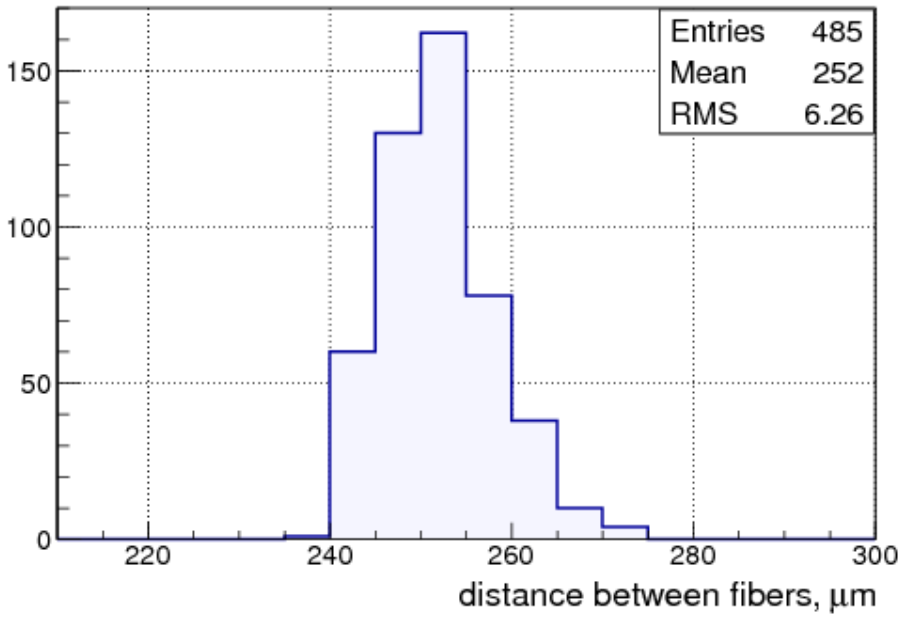

Figure 5: Distribution of the measured distance (in μm) between the centres of adjacent fibres for the sample module shown in Fig. 4.

A dedicated FE electronics chip is being designed for the readout of the SiPMs. The specifications for the signal processing are very dependent on the detector technology and geometry. First studies show that a 5-bit digitization is appropriate while preserving the needed detector resolution. However, specifications for the digital signal processing unit are still evolving, and are dependent on the final detector geometry choices.

As discussed in Sec. 2.1.5, detailed simulation studies will provide information about the optimal geometry of the detector, the channel occupancy in 2.5 m long fibres, and the consequences on the tracking performance. The first results of these studies are expected for Q3 2012, and these will be essential to finalize the design of the fibre modules, of the global detector geometry, and of the FE electronics.

2.1.4 Readout front-end ASIC for silicon strip detectors

Silicon microstrip sensors are being considered for the upgrade of the VELO, TT and IT subsystems. It is therefore crucial for the LHCb upgrade that a FE readout chip suited to this detector technology is developed. The R&D effort has indeed already started. Specifications for the chip design have been devised for the VELO, TT and IT strip detector options. The chip will integrate 128 (or 256) individual readout channels implemented in the IBM 130 nm CMOS technology. From the operational point of view each channel will consist of an AC-coupled analogue FE amplifier-shaper, followed by a 6-bit ADC. The ASIC functionality will include zero-suppression and an interface with the GBT chip [30] that will handle the high speed off-detector data transmission. A slow control block will be part of the design.

Commonalities with a SiPM FE readout chip for scintillating fibres will also be studied. Apart perhaps from the analogue FE part, the two applications might be able to share a large part of the chip design and developments.

A first version of the 6-bit ADC was recently submitted for manufacturing as part of a multi-project wafer. The next protoype will include a front-end design and is scheduled for Q4 2012.

2.1.5 Track reconstruction

The different roles of the three sub-detectors (VELO, TT, Tracker stations) of the LHCb tracking system have been described in the LoI. In this section we report on progress in the implementation of the detector geometry and the pattern recognition software. We focus on studies which will give critical input to technology decisions and the design of the geometry of the tracking detectors.

Track reconstruction in the VELO is a crucial ingredient to the first software trigger level. A first geometry implementation of the VELO pixel detector is available and a pattern recognition algorithm has been developed and tested on a simulated data sample with comparable conditions to those expected at 2×10^{33} cm^{-2}s^{-1}. The reconstruction efficiency is found to be 99.5% for particles which leave a minimum number of hits in the VELO and the Tracker stations. The fake track rate is very low ($< 1\%$) and the processing time of $\sim$ 1ms per event fulfills the stringent trigger requirements. This encouraging study needs to be updated once realistic material estimates are available. The material description depends on the cooling solution and other hardware decisions. The simulation will also take into account a realistic readout-board emulation and clustering algorithm. In parallel, a first software implementation of the VELO strip detector has been developed.

Work on a realistic description of the RF foil in the simulation is ongoing. The XML based description is limited to certain shapes of volumes and thus can only approximately describe the foil. However, both the amount of material and the precise location relative to the production vertex and the first measurement of a particle have significant impact on the impact parameter resolution. Therefore a technique is being developed to import the precise shapes of the CAD foil layouts directly into the GDML format, which is readable by the LHCb simulation. Figure 6 shows a picture of the XML and the GDML description

of the RF foil of the current LHCb detector. It is clearly visible that the GDML version better reproduces the smooth shape of the foil. This new technique allows the detailed study of realistic foil forms.

The impact parameter performance will be dominated by the interplay of three factors: the foil thickness and optimisation of its shape, the radius of the first measured point, and the material contribution of the VELO station providing the first measurement of the track. The role of the simulation will be to optimise simultaneously these parameters, using realistic inputs from the hardware designs as these progress. One further goal of the VELO simulation studies is to optimize the exact location of the VELO sensors along the beam axis.

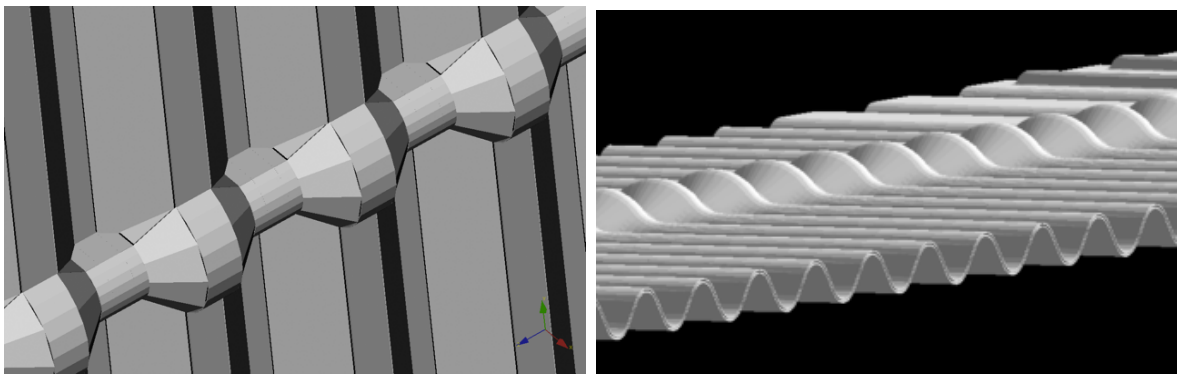

Figure 6: Drawings of the current RF foil descriptions. Left: XML description, which is limited to certain shapes of volumes. Right: GDML description, which import the foil shape directly from the CAD layout.

The task of the Trigger Tracker comprises reconstruction of very displaced tracks (e.g. K^0_S daughters), improvement of momentum resolution of long tracks (tracks which traverse all tracking detectors), fast momentum estimate for tracks used in the trigger made from VELO and TT space points, and reduction of fake (ghost) tracks due to mis-combinations of VELO and Tracker-station track segments. Several features inhibit the current TT detector in performing these tasks. These include the limited acceptance due to a gap at $y = 0$ between the upper and lower detector halves and the beam pipe hole, the very high occupancy close to the beam pipe, the low magnetic field in the TT area and the low redundancy available with 4 layers (two 3D measurements). The TT detector design for the upgrade addresses several of these issues already, e.g. via overlap at module boundaries and finer segmentation close to the beam pipe. The following further potential modifications to the TT layout will be studied with simulation:

- Performance improvements as a function of minimum radial distance from the beam axis;
- Performance improvements as a function of realistic variations of the magnetic field at the detector location;

- Performance improvements including two additional planes in the intermediate tracking volume.

Implementing these potential changes might require significant technical modifications, e.g. in the support structure of the beam pipe. Thus any potential improvement must be well motivated by performance software studies surveying all tasks of the TT detector simultaneously. A first implementation of the TT upgrade geometry is available to start these studies.

Two pattern-recognition algorithms are used for reconstructing the tracks in the Tracker stations. One uses VELO tracks as input; the second one performs a standalone search in the Tracker stations. While the first one, exploiting VELO track information in the pattern-recognition phase, turns out to be more robust in high occupancy events, the second one is necessary for reconstructing decay products of long-lived particles such as K^0_S, which decay outside the VELO. Thus any optimization of the geometry layout of the Tracker stations needs to consider both algorithms. Work is ongoing to adapt the current algorithms to deal with the new geometry.

Each of the three current Tracker stations is sub-divided into 6 regions, which correspond to the two OT halves and the four IT boxes. Most of the tracks in the Tracker stations cross the same region in all three stations. This is heavily exploited in the pattern recognition to reduce combinatorics when combining measurements from x and u/v layers. The CT proposal consists of two detector halves only, but profits from the significantly better resolution compared to the current OT. To test the impact on combinatorics in the pattern recognition is one of the major tasks of the ongoing CT simulation efforts.

The alternative proposal for the Tracker stations consists of an enlarged silicon Inner Tracker combined with OT straw tube modules. For this layout, it is important to study the required size of the IT to keep the occupancy of the straw tubes at a reasonable level. In the current LHCb detector the IT layers are in front of the OT layers. A realistic material description of the IT is needed to estimate the gain in terms of OT occupancy due to secondaries from material interactions, when the order of IT and OT is inverted.

It is likely that the number of u/v layers can be reduced from 6 to 4, which would result in less material and thus in less multiple scattering. Pros and cons will be studied for both Tracker-station technologies and both pattern-recognition algorithms.

2.2 Particle identification

2.2.1 RICH system

In the upgrade the upstream RICH-1 detector will retain its current C_4F_{10} gas radiator, however the high occupancies mean that the aerogel radiator will be removed. The downstream RICH-2 CF_4 gas radiator will remain unchanged. The HPD photon detectors and readout electronics will be replaced by multi-anode photomultipliers (MaPMTs) with external new 40 MHz readout electronics. The photon-detector mounting frames to house the MaPMTs and their local magnetic shielding will be re-designed and replaced. All the remaining RICH mechanical and optical components will be re-used as much as

possible. An R&D programme has been embarked on to evaluate all the upgraded RICH technology choices. The LHCb Monte Carlo is now able to incorporate MaPMTs in the RICH description and performance studies are underway.

The baseline MaPMT photon detector is currently under test. We estimate that 1152 MaPMT units will be required to equip RICH-1 and 2560 to equip RICH-2. This gives approximately 238k readout channels in total. Following laboratory characterisation, already well advanced, the MaPMT will be tested in a prototype RICH detector in a CERN test-beam in autumn 2012. Based on these studies the final decision will be made in December 2012 to confirm the MaPMT as the upgrade RICH photon detector.

The MaPMT readout must conform to the upgraded 40 MHz LHCb electronics architecture. The front-end (FE) chip will be an ASIC which provides the shaping and amplification as well as discrimination and digitisation of the MaPMT signals. A prototype FE electronics 4-channel readout chip, now named the CLARO-CMOS, has been fabricated, initially in 0.35 μm-CMOS technology. The prototype has been tested with single photons sent to a MaPMT pixel and shows a pulse fall-time restored before 25 ns, thus eliminating possible spill-over/dead-time effects for LHC operation. The CLARO-CMOS will be expandable to 8 or 16 channels in a later iteration. As a parallel activity, we are evaluating the Maroc-3 readout chip. Simulations will be made to investigate whether the Maroc-3 shaping time is compliant with the expected maximum occupancy and whether spillover/dead-time effects are tolerable. The decision on which final readout chip to use will be taken after test-beam operation and radiation testing, and is a major milestone scheduled for June 2013.

All FE decision logic will be implemented in on-detector readout boards; studies are underway to determine the optimum geometry, number and functionality of these boards. The boards will include commercial FPGAs and be used to set up the FE chip, supervise the triggering, and format and (possibly) zero-suppress the data. The FPGAs must also be proven to resist the radiation in the vicinity of the RICH photodetector planes. The on-detector boards will use the new generation of radiation hard giga-bit optical link (GBT) chipset [30] to interface with the Versatile Link optical readout. The modularity of the MaPMT modules has an important bearing on the overall design philosophy and cost of the on-detector boards, the optical links and the off-detector readout modules. A decision on module modularity will be made in December 2012.

With the absence of the RICH-1 aerogel radiator, in principle the photodetector plane of RICH-1 can be significantly reduced in area from the existing detector, resulting in an overall cost saving. Whilst the default option is to retain the current RICH-1 geometry, studies to verify that occupancies are tolerable in the innermost regions are still on-going. It has already been confirmed through simulation that occupancies in the inner regions are very high (well above 10%) and therefore a modification of the RICH-1 optics is also considered. In this arrangement, replacement of the carbon-fibre mirrors would spread the C_4F_{10} rings over a greater number of MaPMTs. We will also address the issue in RICH-1 of poor accessibility of MaPMTs in case of their failure (especially in the high-occupancy inner regions where the risk of photon loss could be substantial). Modifications of RICH-1 in this way would increase the scope of the project; a decision on the RICH-1

optical system will be taken at the end of 2012, following simulation studies.

The current schedule, independent of RICH-1 optical modification, plans the RICH Technical Design Report in November 2013. Construction would start in January 2015 and the final population of the MaPMT modules would be complete at the end of 2017.

In the LoI we proposed that the RICH system would also be augmented by the TORCH, a novel detector based on time-of-flight to identify low momentum particles below $\sim$ 10 GeV/c. The R&D funding for this detector has been the subject of a successful 4-year EU grant award which will start in June 2012. Assuming an effectual R&D period, a TDR addendum will be submitted to the LHCC in May 2016, proposing the TORCH detector to be part of a staged programme for later installation in the LHCb detector.

2.2.2 Calorimeter system

The main challenge of the calorimeter upgrade is to replace the current front-end electronics by a new system able to send data to the DAQ at 40 MHz. Moreover, the new electronics must have a gain five times higher than the present system, in order to compensate for a gain reduction that will be imposed on the photomultipliers so that the mean anode current remains at an acceptable level during high-luminosity running. This requirement has implications for the maximal acceptable noise level for the analogue components. Two analogue implementations based either on the ICECAL[31] ASIC or on discrete components are already at an advanced stage of design. The digital front-end is being developed in parallel and is based on the ACTEL A3PE flash-based FPGA and on the GBT[30] ASIC from CERN. The first common tests of both the analogue and digital parts began at the end of 2011 (see Fig. 7). The choice of which analogue solution to adopt will be made by mid-2013, following beam and radiation tests. Then, a new prototype merging both the analogue and the digital parts on a single board will be designed. A final prototype will follow, with the full target number of 32 channels per board.

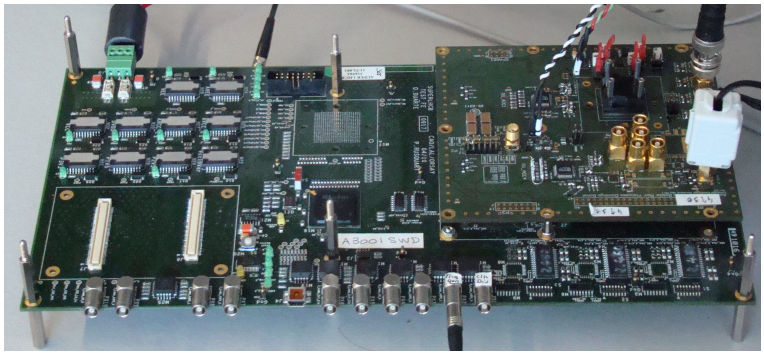

Figure 7: The digital mother board and the analogue mezzanine prototypes described in the text. The A3PE FPGA is visible on the digital part. The analogue part supports the discrete component implementation and the ICECAL ASIC (maintained on the PCB of the mezzanine with the black support at the top right).

Many elements of the current calorimeter electronics will be retained for the upgrade: the trigger validation boards (TVB), which will be re-used by the Low Level Trigger; the LED calibration system; the high voltage control; the photomultiplier current measurement system etc.. The slow control of these elements is based on the SPECS system [32]. Depending on the element, the control is effected either through a dedicated FPGA (e.g. for the TVB located in the front-end crates) or through SPECS mezzanines (e.g. the high-voltage control). Development is underway to make both solutions compliant with upgrade operation, and common tests are scheduled for early 2014.

The Scintillating Pad Detector (SPD) and the Preshower (PRS) of the current detector will most probably be removed for the upgrade. Although the removal of this system is expected to lead to some loss in particle identification performance at low p_{T}, partial compensation will come from an improved energy resolution in the ECAL itself, on account of the reduction in material before the detector. The role that the SPD/PRS system plays in the current L0 trigger is not considered essential for the Low Level Trigger of the upgrade. A final benefit of the removal is that the calorimeter calibration will be more straightforward without the SPD/PRS in place. Simulation studies are ongoing to confirm this decision.

Radiation damage is a concern for the innermost modules of the electromagnetic calorimeter, where the dose leads to a degradation of the constant term in the resolution from a non-uniform attenuation of the light collected along the modules. In order to improve understanding of this issue, two test models were installed directly in the LHC tunnel in 2009, in a position where they accumulate approximately five times the radiation dose of the modules in the innermost region of the ECAL. During the 2011-12 shutdown scans with a radioactive source were used to characterise these test modules and no significant degradation was observed. These studies will be repeated after further irradiation. Spares are available should it be found necessary to replace the modules in the centremost part of the inner region.

2.2.3 Muon system

In the LHCb upgrade, station M1 of the muon system will be removed and the critical question then concerns the rates in stations M2-M5. The current system was designed in order to stand incident particle rates up to 1 MHz per front-end channel without any loss of efficiency due to space charge effects and without any degradation of the time resolution [33]. The rates expected from simulation at $1 \times 10^{33}\,\mathrm{cm}^{-2}\mathrm{s}^{-1}$ and $\sqrt{s} = 14$ TeV are all below this value [1]. Recent studies with real data indicate that the measured particle rates in the muon system scale linearly with luminosity and agree well with simulation, apart from for the innermost regions of stations M2 and M3 where the Monte Carlo underestimates the rates in data by around 50%. It is therefore concluded that at nominal upgrade luminosity the rates in the muon system will be tolerable, and so only minimal modifications will be necessary, in order for the readout to comply with the new DAQ and trigger scheme. These modifications remain essentially unchanged from those described in the LoI [1]. A TDR is scheduled for Q3 2013.

Considerations about the aging of the MWPC of the Muon system have also to be taken into account in view of the system upgrade. The LHCb MWPCs have been proven to stand an integrated charge under irradiation up to 0.45 C/cm of wire [34, 35]; this, however, is only about 70% of the maximum integrated charge expected in the inner region of station M2, over the 50 fb^{-1} of integrated luminosity foreseen for the upgrade. Therefore, it is important to test the behaviour of the MWPCs at integrated charges approaching 1 C/cm. Moreover, to cope with possible aging effects that can arise during the upgrade data taking period, additional spare chambers will be constructed.

If it is decided to operate LHCb at the higher luminosity of $2 \times 10^{33}\,cm^{-2}s^{-1}$ then new solutions will be required in order to deal with, in particular, the problems that will arise from detector rate limitations and electronics dead-time in the inner regions of the M2 and M3 stations. One possibility would be to go from a combined wire/cathode readout with FE-channels reading out a surface area of about 15 cm^2, to a simple cathode readout with pads of a smaller size, thus minimizing the rate effects. Simulation studies are planned to optimize the required granularity. Investigations of candidate technologies to implement this solution are proceeding in parallel. The possibility to design and develop new faster front-end electronics is also under investigation. This solution, by reducing the dead time, would allow more flexibility in the optimisation of the detector granularity. Finally, the increased rate could be suppressed by installing additional shielding downstream of the hadron calorimeter in front of the M2 inner region. All of these approaches are under consideration. Further shielding improvements are also foreseen behind M5, where recent results obtained from data indicate that particles back-scattered from an LHC magnet just downstream of the muon system may lead to inefficiency due to dead time. This specific problem can also be tackled by modifying the logical combination of readout channels in the outer part of M5. Both approaches will be pursued, guided by the results of simulation studies.

2.3 Data processing

The task of the data processing concerns the transport of the data from the output of the FE electronics up to their reconstruction. It encompasses data acquisition, trigger and computing.

2.3.1 Data acquisition and trigger

The readout board is one of the key components of the data processing. The so-called TELL40 interfaces the FE electronics with the online network. The board collects event fragments at 40 MHz and merges them into packets of a local area network technology. The packets are sent to the event processing farm via a fast network based on a standard protocol for which 10 Gigabit Ethernet is the favoured option. In this system, timing and fast control (TFC) as well as slow control (ECS) have to be distributed to each readout board as well as to the FE electronics. The main evolution since the LoI is the use of the same generic board to satisfy all the requirements for data transmission, TFC and

ECS. This takes advantage of the high density of serial links available in state-of-the-art Stratix V FPGAs which also offer many resources for the local data processing. We have decided to implement this hardware using the ATCA standard [36]. This follows trends in industry and HEP, and we will benefit from ATCA evaluations planned at CERN as well as developments in other experiments. The first full-size prototype is expected by the end of 2012 with which we aim to validate serial links running at 10 Gigabit/s, investigate the FPGA resources required by the most demanding processing and gain experience of the ATCA standard.

The upgraded LHCb read-out system aims at a trigger-free read-out of the entire detector at the bunch-crossing rate of 40 MHz. In order to adapt the network and event-filter farm capacity to the available resources the existing Level-0 hardware trigger will be upgraded and adapted to become the Low Level Trigger (LLT) [1], which allows a smooth variation of the input rate to the farm between 1 MHz and 40 MHz. The main parameters that define the trigger as well as the size of the data processing, for the start-up in 2019, are those specified in the LoI: the rate of colliding bunches with at least one interaction at the input of the event filter farm will be 10 MHz, the output rate of the event filter farm will be 20 kHz, the event size will be of the order of 100 kB. A key aspect of this design concerns the transformation of the current Level-0 into the LLT. The integration of the current hardware in the new readout architecture will be done using a unique hardware unit, the readout board. Development of High Level Trigger (HLT) software is also critical for the upgrade, since the HLT must run the tracking algorithm, the reconstruction and the event selection for many different channels in a very demanding real-time environment. A team of physicists and computing experts will be set up to develop very flexible software, minimising processing time and the use of real-time computing resources. The HLT must follow the maturation of the detector keeping very high trigger performance.

Another key component is the online network for the upgrade. The readout network must be able to connect approximately 4000 10-Gigabit/s input ports with up to 5000 compute nodes. The challenge in the network design is to come up with a cost-effective solution for a large multi-Terabit/s network. We are investigating two network technologies: Ethernet and InfiniBand. The architecture will use either large core-routers with deep buffers or cheap switches with short buffers. The former implementation is more expensive but minimises the traffic management and the need for buffering in the readout boards. The latter requires more sophisticated traffic management and more buffering in the readout boards. Studies and prototyping are ongoing to arrive at a decision in 2015.

2.3.2 Computing

The computing covers several domains: the workload management system, the framework, the simulation, the reconstruction applications, as well as the daily operation for data reconstruction and stripping. Some of these software and applications will run in a very demanding context in the event filter farm.

As regarding simulation we have already organised activities to identify an upgrade simulation coordinator and a geometry support person, as well as one person in each

detector group responsible for the detector specific software.

Concerning other aspects of the computing, additional manpower is required to take responsibility for R&D and implementation of several tasks including: (i) development of the distributed computing and workload management system for high rate; (ii) use of Cloud services; (iii) parallelisation of LHCb applications within the framework, and efficient use of many core processors; (iv) databases with high throughput; (v) code developments needed for software to run on the event filter farm. We estimate of the order of 10 FTE per year are required. We will organise this activity by identifying an upgrade computing coordinator in the coming months, who will set up and coordinate a team of developers with specialised skills in order to start the R&D as soon as possible. Although the computing project is a common project supported by all institutes, we would like to be able to attribute the responsibilities for key domains of the software development to specific institutes as we usually do for the sub-detectors. Experts from CERN, France, Romania, Spain and UK have already expressed their interest, and other countries are planning to join these activities in the near future. The required manpower is expected to be available and acknowledged by the collaboration, and will be defined in more detail in the computing TDR.

The hardware resources needed have been estimated at first pass, and this estimate will be refined in the next years. These resources will be requested in due time via the WLCG, in the usual manner.

2.4 Safety

New sub-systems and equipment installed for the upgrade will follow the CERN safety rules and codes, CERN safety document and European and/or international construction codes for the structural engineering as described in EUROCODE3. Initial safety discussion will be held well before the release of the Technical Design Reports. Estimates of the radioactive waste that will be produced are being calculated, and the results will be presented in the TDRs.

3 Schedule, costs and interest of institutes

3.1 Schedule

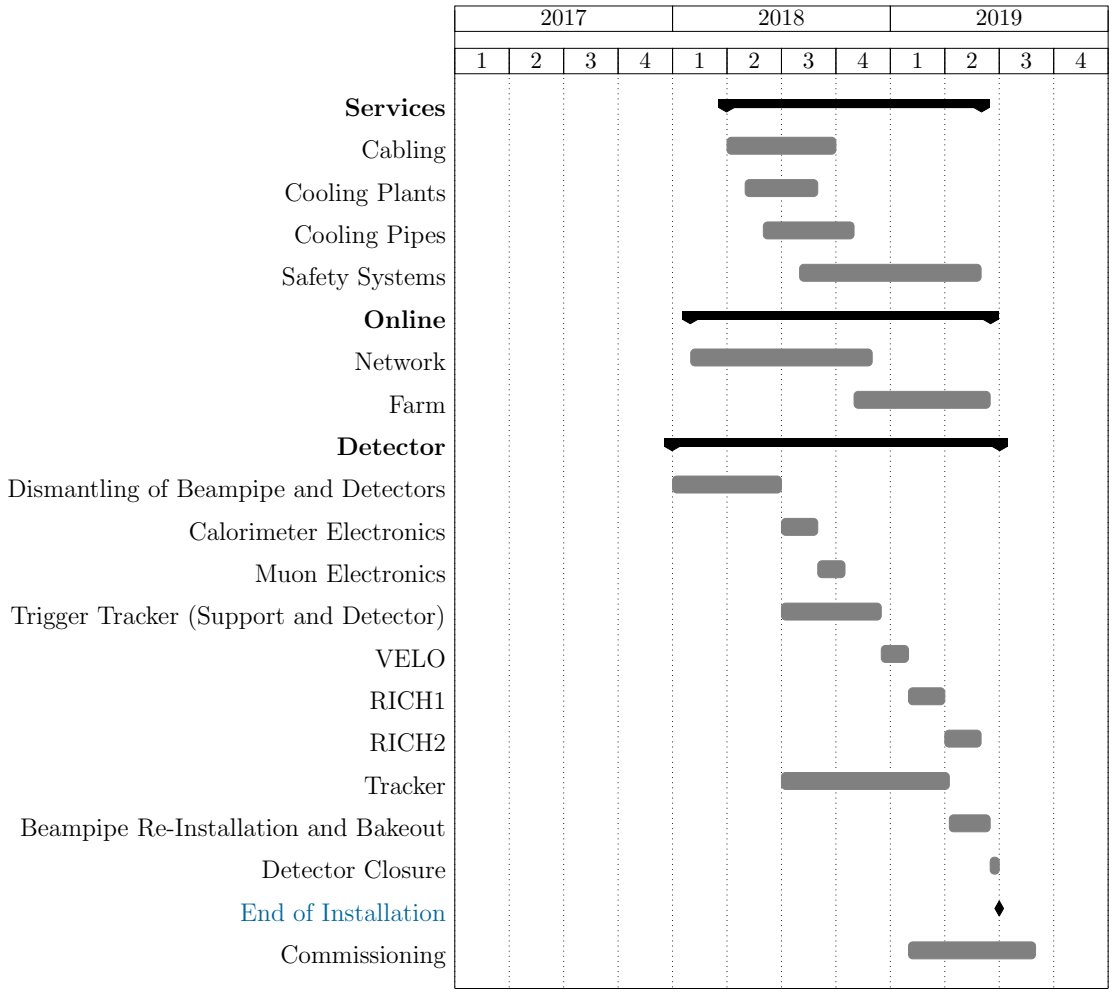

Figure 8: Project schedule for installation.

The installation of the LHCb upgrade takes into consideration the present long-term planning of LHC and will start with the long shutdown (LS2) in 2018. The overall time for the installation and commissioning of the LHCb upgrade amounts to 18 months (Fig. 8). It is mandatory that the new detector systems are assembled as much as possible before the installation. Some systems will be integrated in the existing supports and infrastructure. The assembly of these systems can take place only once access to the cavern is granted.

LHCb will profit as much as possible from the first long shutdown (LS1) and any intermediate extended technical stop before 2018 to prepare the installation of the upgrade.

The installation of the LHCb upgrade will start with the opening of all detector systems and the removal of the beam pipe and systems that will not be used in the future. In

the baseline scenario, the first muon station (M1) will be dismounted and probably the PreShower (PRS) and Scintillating Pad Detector (SPD) as well. This will be followed by the dismantling of the Tracker systems to allow the modification and adaptation of the support structures for the new systems to be integrated.

The individual sub-system schedules take account of the R&D, engineering and production period, the assembly and start of installation. The most important milestones such as the technology choice, publishing of the TDR, engineering design review (EDR) and production readiness review (PRR) are embedded in the system schedules.

Most of the TDRs of the sub-systems will be issued towards the end of 2013, after the technical choice for the baseline has been taken. For the sub-systems which will exploit COTS (commercial off-the-shelf) items, production time is a less critical consideration and hence the TDRs of these systems will be submitted later in order to profit as much as possible from further developments.

The R&D work on the VELO will continue for both options until the EDRs and the preparation of the TDR end of 2013 as illustrated in Figs. 9 and 10.

The decision between an Outer Tracker with straw tubes together with a Central Tracker made of scintillating fibres and SiPMs, or an OT with a larger Inner Tracker of silicon technology, will be taken by mid-2013, before delivering the Tracker TDR (Figs. 12, 13, and 14). In both cases a modification to the existing support structures and services will be required. This will be the case for the Trigger Tracker as well. The schedule for the R&D studies, reviews and production time for the Trigger Tracker are given in Fig. 11.

The schedule for the RICH detectors is given in Fig. 15. The new photon detectors require a different mechanics for both systems. The calorimeter modules will stay untouched and the efforts will mainly be invested in the development and production of new electronics (Fig. 16). Some of the muon chambers will have to be exchanged during the upgrade data taking and therefore a stock of modules will be produced. Concerning the electronics, the principle task will be the development of the firmware for the readout board once the electronics board is available (Fig. 17).

All sub-system schedules are coherent with the general electronics milestones shown in Table 4. The main R&D work for the Online project is to evaluate the different technolgies available. As most parts will be COTS products, the Online TDR is scheduled for early 2016 (Fig. 18).

Milestone	Date
Readout Board	
Preseries production	Q12 2014
Series Production	Q34/2014 – Q34/2015
LLT integration	Q12/2016 – Q34/2017
Commissioning	Q12/2018 – Q34/2018
GBTX	
Prototype for tests	Q1/2013
Launch production	Q4/2013
First parts available	Q2/2014
Versatile Link	
Prototype for tests	Q4/2012
Pre-series production	Q4/2014
Production completed	Q4/2015

Table 4: General electronics milestones.

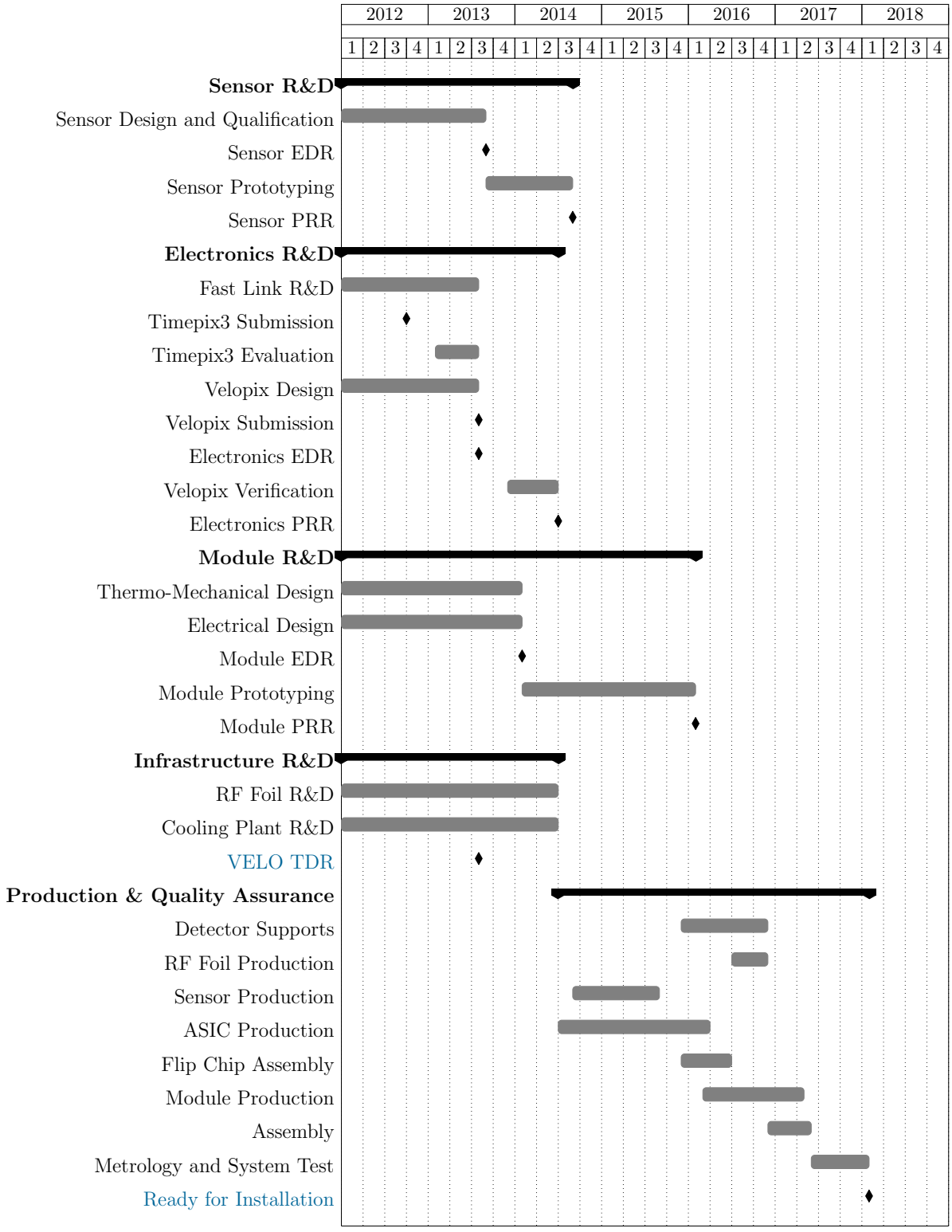

Figure 9: Project schedule for Vertex Locator (pixel option).

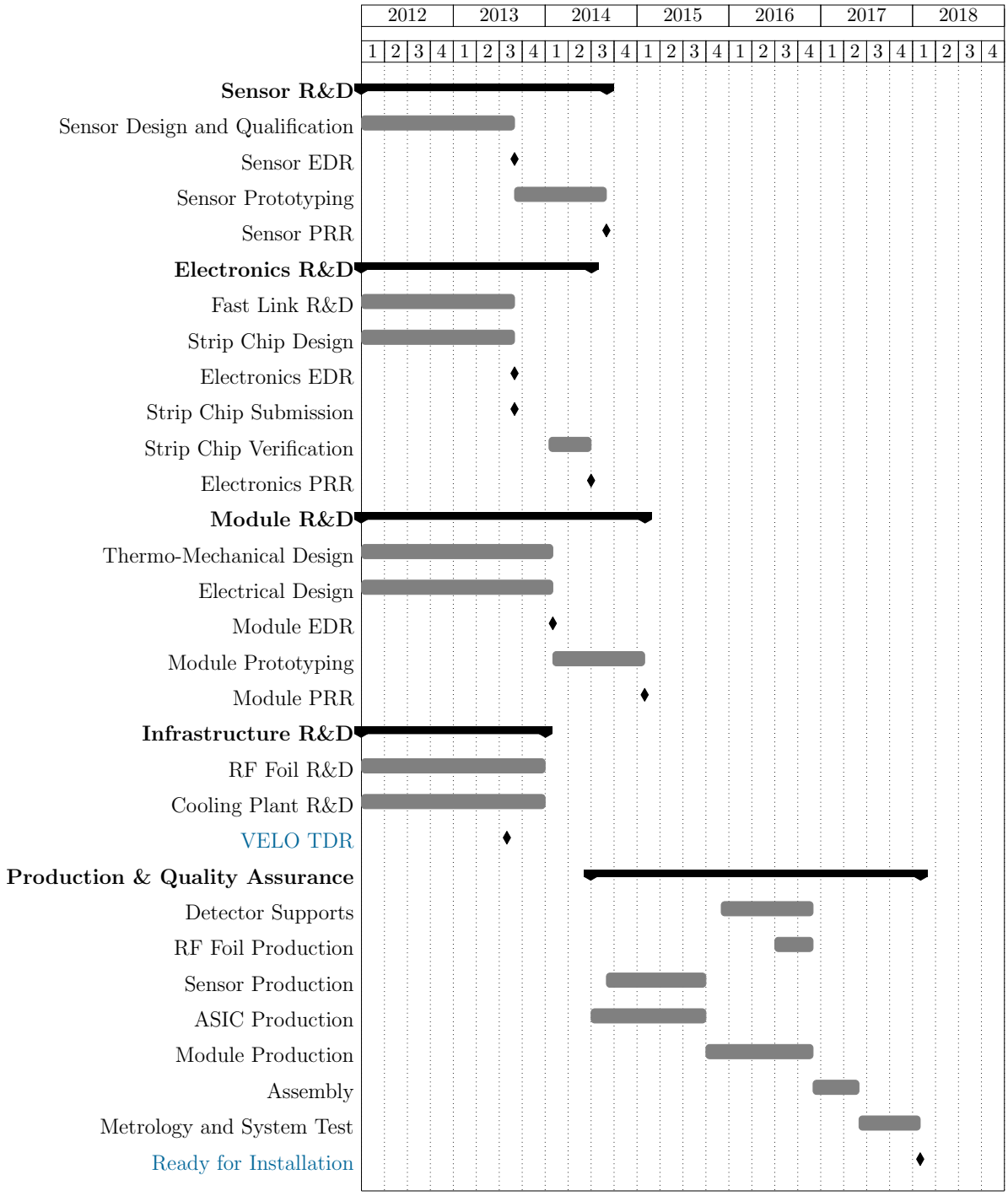

Figure 10: Project schedule for Vertex Locator (strip option).

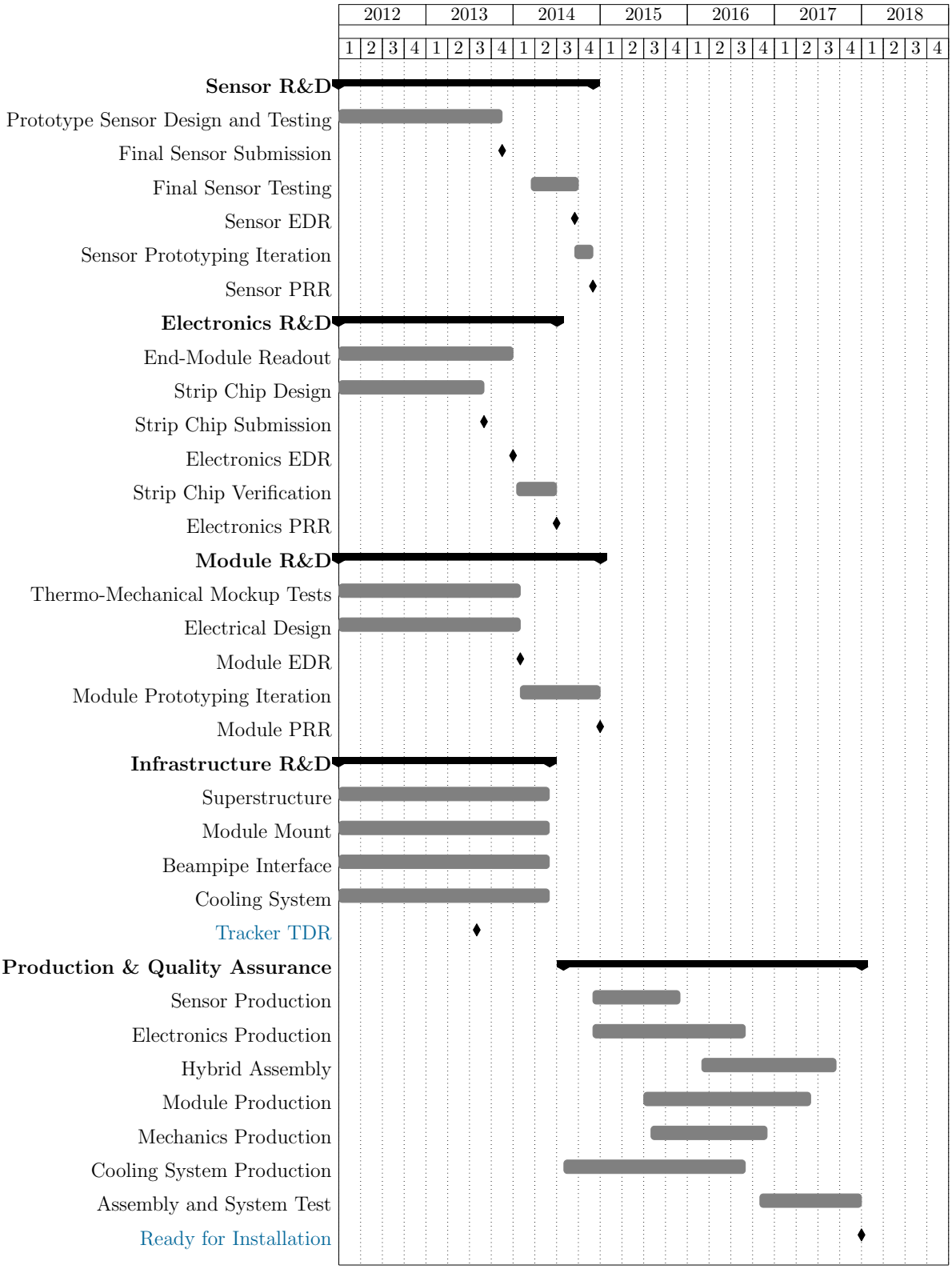

Figure 11: Project schedule for Trigger Tracker.

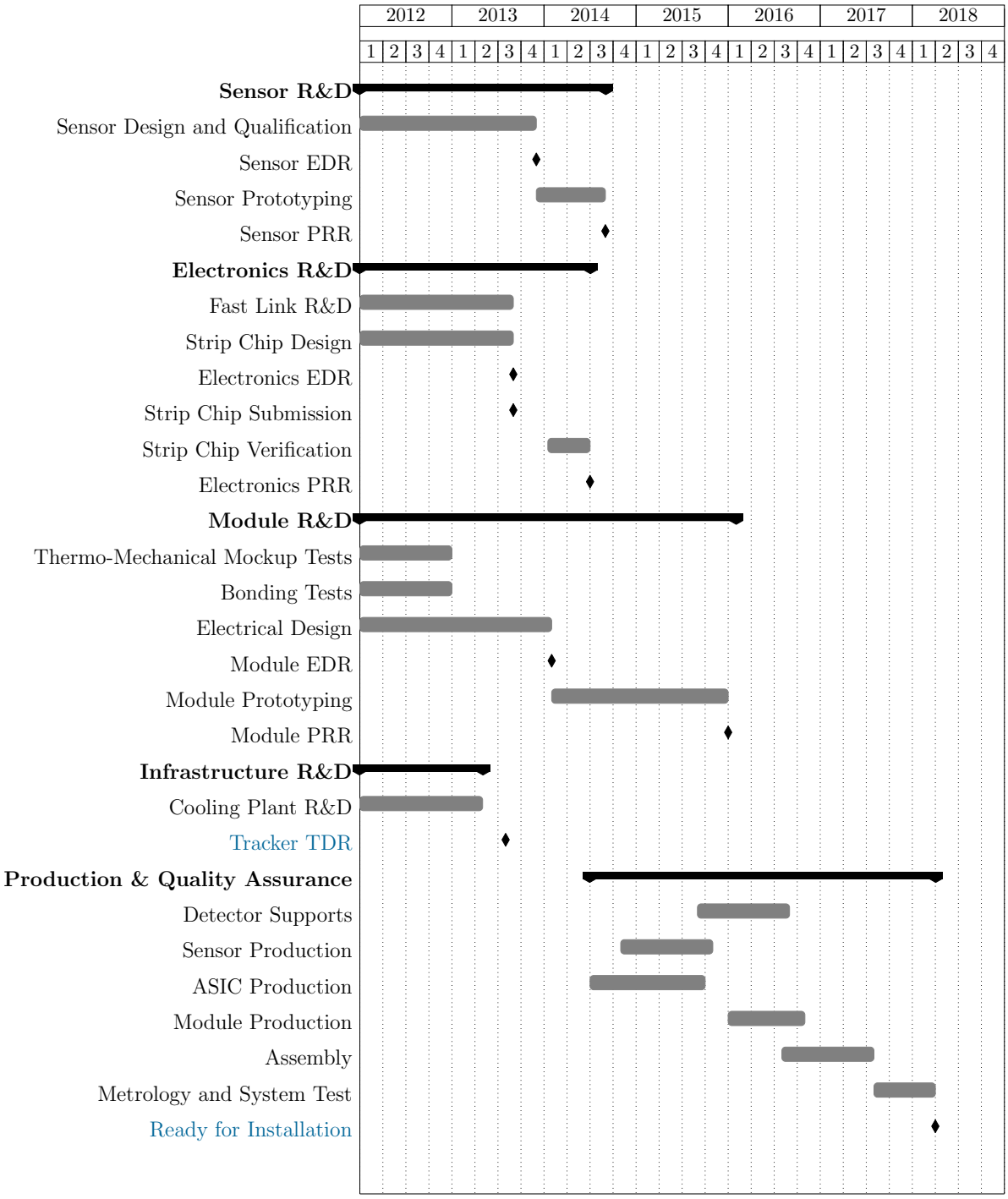

Figure 12: Project schedule for Inner Tracker.

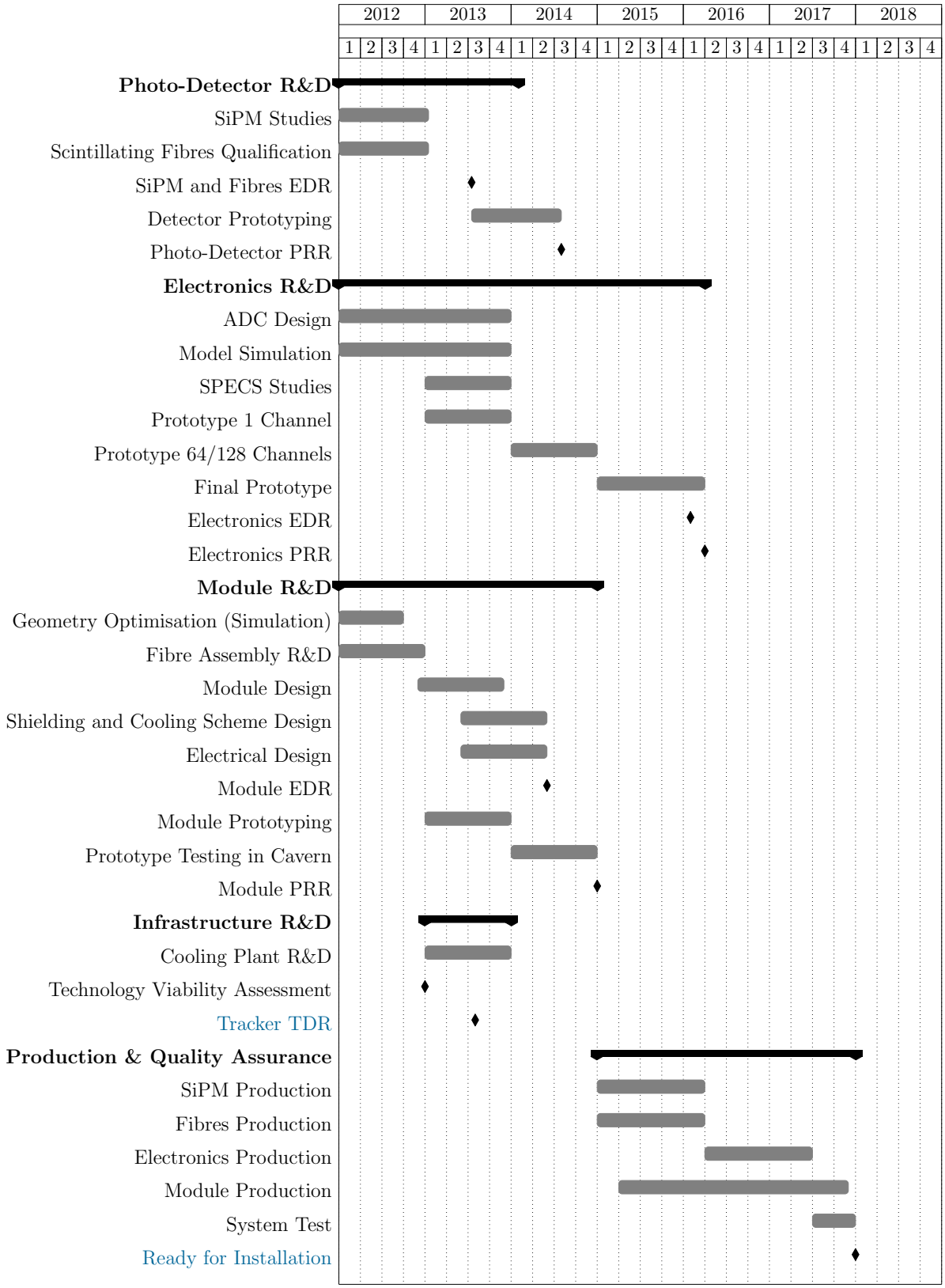

Figure 13: Project schedule for Central Tracker.

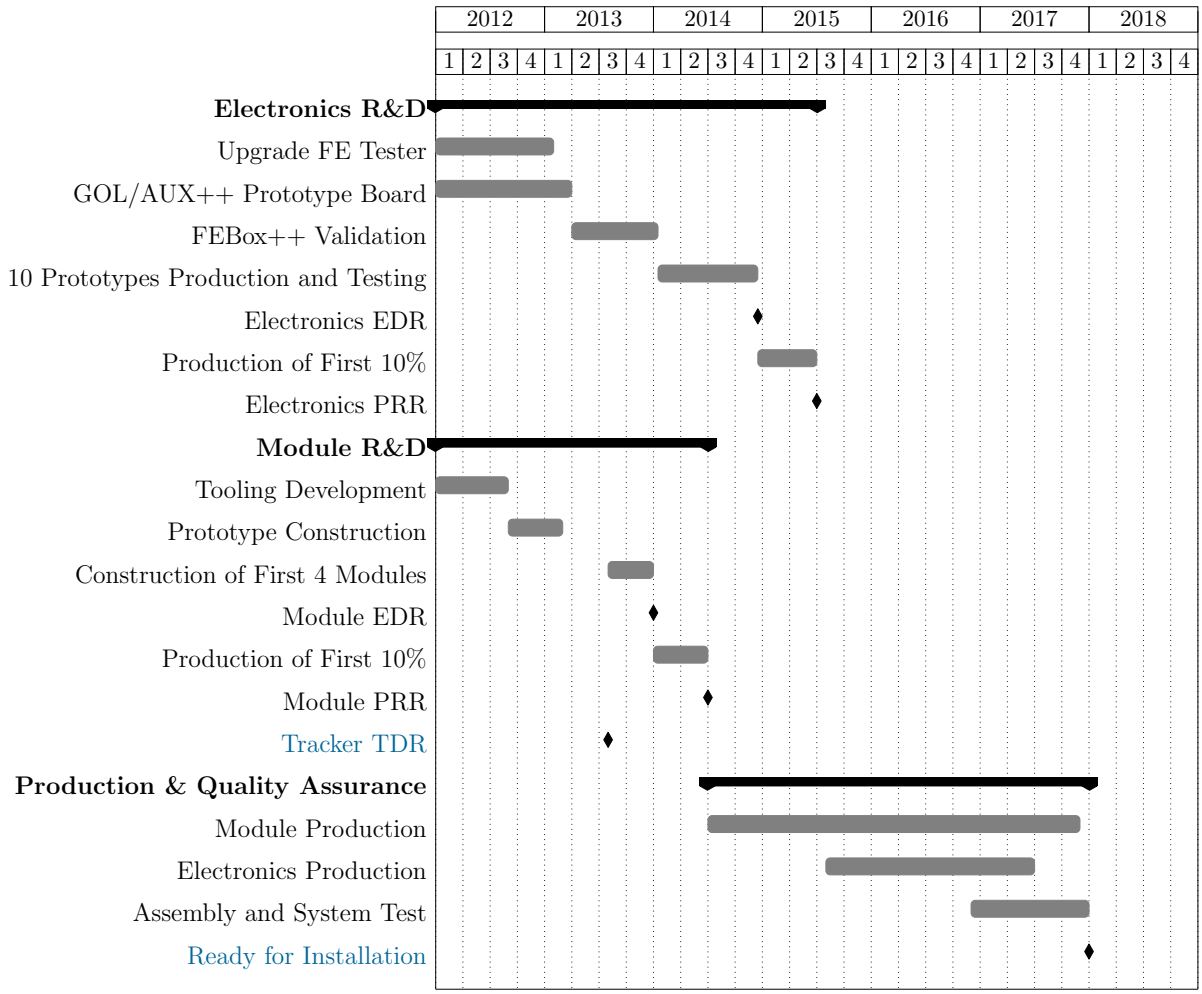

Figure 14: Project schedule for Outer Tracker.

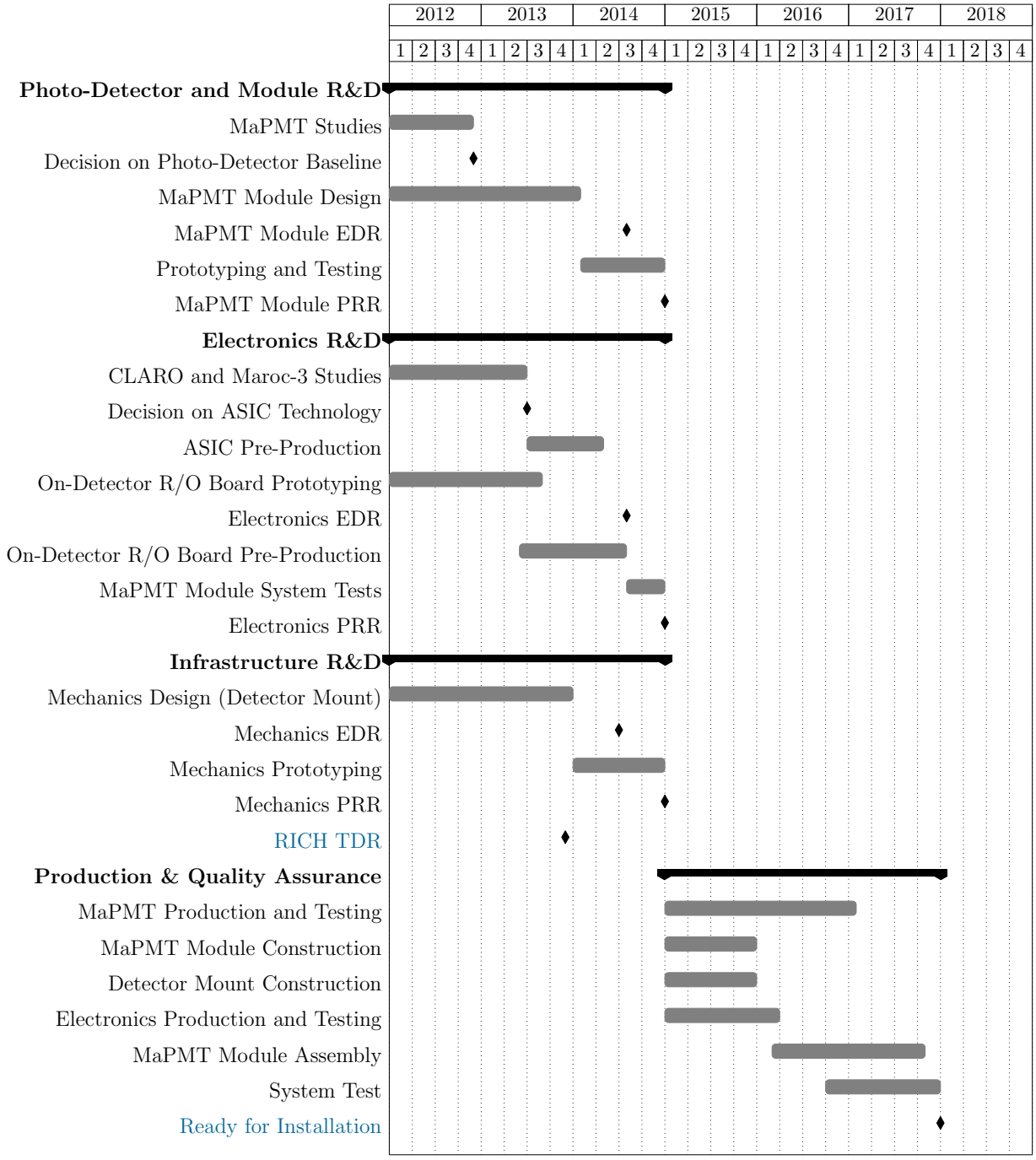

Figure 15: Project schedule for RICH.

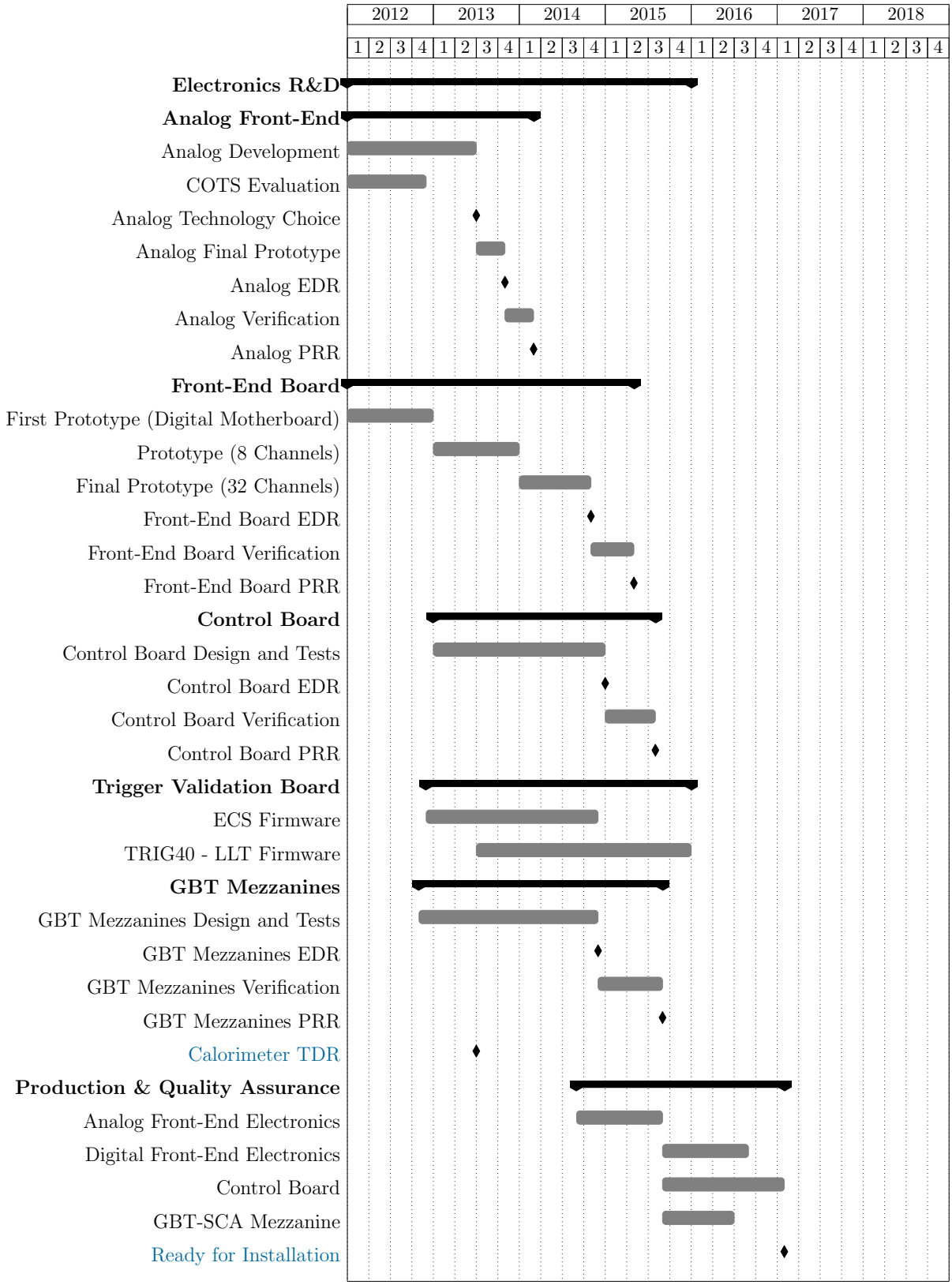

Figure 16: Project schedule for Calorimeter.

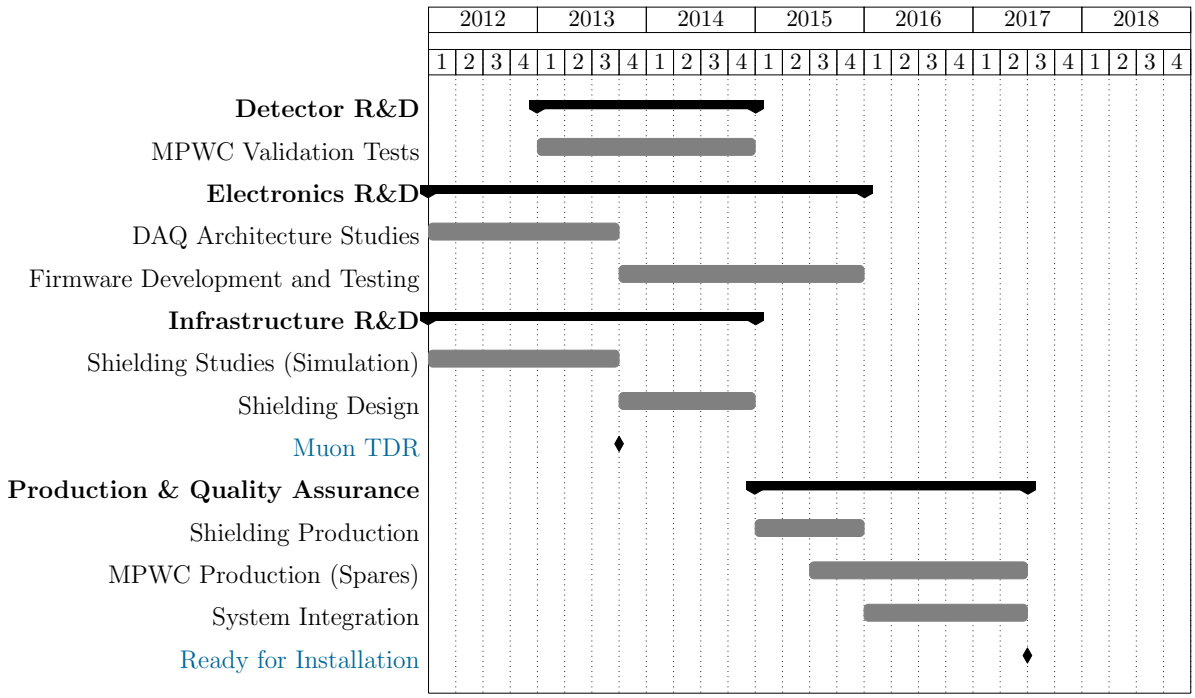

Figure 17: Project schedule for Muon System.

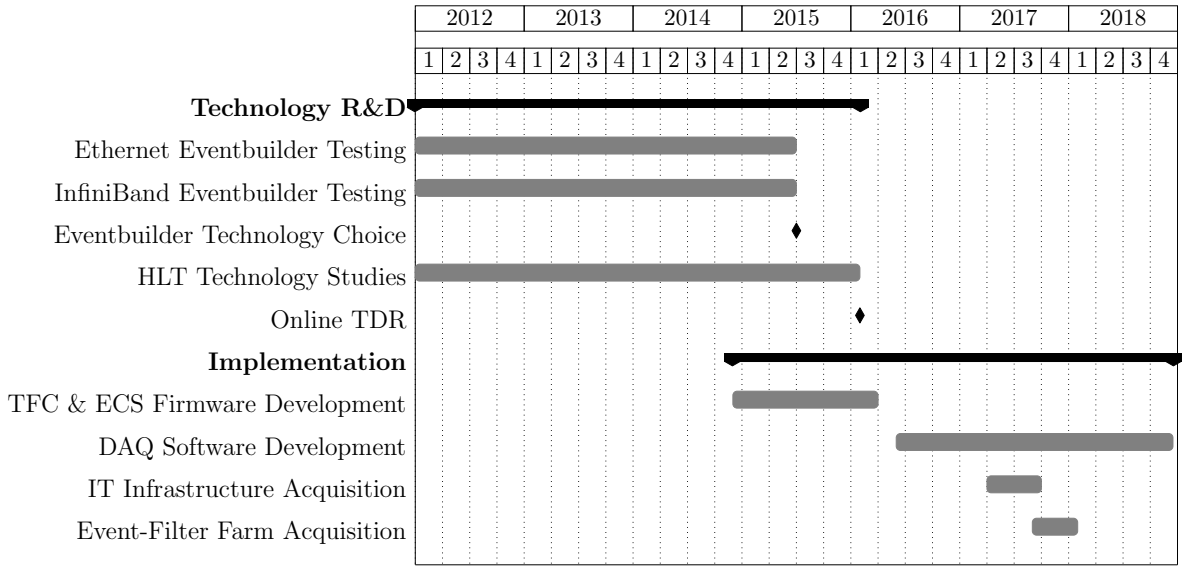

Figure 18: Project schedule for Online.

Vertex Locator		Cost [kCHF]	
		Pixels	Strips
Detector		935	1050
	Sensors	345	460
	Flex Hybrid	300	300
	Module Cooling	290	290
Electronics		3460	2445
	Front End	1420	410
	Optical Links	425	420
	Readout Board	700	700
	General Electronics	345	345
	High-Speed Cables	570	570
Infrastructure		1035	1035
	RF Foil	460	460
	Motion, Vacuum, Cooling	575	575
		5430	**4530**

Table 5: Cost estimates for Vertex Locator.

Trigger Tracker		Cost [kCHF]
Detector		3060
	Sensors	2300
	Hybrids & Connectors	760
Electronics		2595
	Silicon Strip RO chip	900
	Front End	450
	Optical Links	345
	Readout Board	740
	General Electronics	160
Infrastructure		560
	Support Structure	230
	Cooling	330
		6215

Table 6: Cost estimate for Trigger Tracker.

3.2 Cost

In the following we present the detailed cost estimates of the individual sub-systems, as well as the cost of the Common Projects.

As far as the sub-systems are concerned, at this stage we have several technology

Inner Tracker		Cost [kCHF]
Detector	3760	
	Sensors	3150
	Hybrid & Flex	610
Electronics	1210	
	Front End	300
	Optical Links	140
	Readout Board	230
	General Electronics	540
Infrastructure	380	
	Mechanics	230
	Cooling	150
	5350	

Table 7: Cost estimate for Inner Tracker.

Central Tracker		Cost [kCHF]
Detector	2880	
	Fibres	1100
	Silicon PM	1500
	Modules	280
Electronics	4020	
	Front End	1550
	Optical Links	800
	Readout Board	1270
	General Electronics	400
Infrastructure	960	
	Support Structure	270
	Cooling	390
	Shielding	300
	7860	

Table 8: Cost estimate for Central Tracker.

options for the detector upgrade and therefore the cost evaluation is given in Tables 5 to 13 in kCHF for each option separately, including a contingency of 15%. The cost of both technologies for the VELO, the pixel and strip solution, are given separately in Table 5. The existing vacuum vessel of the present VELO will be reused, but a new RF foil will be required. The current cooling system will need some modification to provide sufficient cooling power to the new detector. The Trigger Tracker cost estimates are based on a solution with four planes with a finer segmentation in y compared to the existing TT

Outer Tracker		Cost [kCHF]			
		IT Option		CT Option	
Detector		1680			
	Straws		760		
	Panels		430		
	Spacers & Wires		490		
Electronics		3610		2000	
	Front End		1840		900
	Optical Links		250		200
	Readout Board		1400		780
	General Electronics		120		120
Infrastructure		410			
	Structure adaptation		285		
	Mechanics		125		
		5700		**2000**	

Table 9: Cost estimates for Outer Tracker.

RICH		Cost [kCHF]	
Detector		6170	
	Photon Detector		6170
Electronics		2845	
	Front End		1140
	Optical Links		845
	Readout Board		700
	General Electronics		160
Infrastructure		420	
	Photon Detector Support		400
	Mu-Metal Shield		20
		9435	

Table 10: Cost estimate for RICH.

(Table 6). The silicon technology for the VELO strip, Trigger Tracker and Inner Tracker will profit from the common project of the Silicon Strip RO chip and the total cost for this is included in Table 6. For the Outer Tracker the number of FE electronics boards that need replacement for the 40 MHz readout depends on the technology choice of the Tracker system. The cost for the Inner Tracker is given for the 2-ladder option (Table 7). The 3-ladder option would have an identical number of read-out channels and its cost would simply increase proportionally to the increase in sensor surface. In case the Inner Tracker with a silicon strip solution will be selected, short Outer Tracker modules will have to be

Calorimeter		Cost [kCHF]
Electronics	1905	
	Front End	690
	Optical Links	410
	Readout Board	660
	Controls Board	65
	ECS Mezzanine	50
	Crates	30
	1905	

Table 11: Cost estimate for Calorimeter.

Muon System		Cost [kCHF]
Detector	345	
	Chamber Material	345
Electronics	1270	
	Optical Links	45
	Readout Board	1015
	General Electronics	210
Infrastructure	230	
	Shielding	230
	1845	

Table 12: Cost estimate for Muon System.

built. On the other hand, if the scintillating-fibre Central Tracker were to be selected, with the cost as summarized in Table 8, less of the new FE electronics for the OT would be required. The cost for the OT modules and full electronics production are given in Table 9. The main structure of both RICH detectors and its optical equipment will stay untouched. The cost table for the RICH systems (Table 10) shows the budget required for the production of new photon detectors, their mechanical support and 40 MHz readout electronics. The Calorimeter (Table 11) requires new front-end electronics to cope with a

Trigger & Readout System	Cost [kCHF]
Readout System	1495
Low Level Trigger	345
	1840

Table 13: Cost estimate for Trigger and Readout System.

Common Projects		Cost [kCHF]
Online	11170	
	Readout Network	4940
	Controls Network	905
	Controls System	930
	PC Farm	3125
	Infrastructure	770
	Timing & Fast Control	500
Common Electronics	2000	
	Optical Fibres & Connectors	500
	Common Spares	700
	Power Supplies, Crates, Racks	450
	DC-DC Converter	350
General Infrastructure	2500	
	Civil Engineering, Building	450
	Cooling & Ventilation	380
	General Assembly	230
	Electrical Power Supply	110
	Radiation Shielding	200
	Survey	120
	Long Distance Cabling	590
	Safety	300
	Gas and Fluids Piping	120
	15670	

Table 14: Cost estimate for Common Projects.

data acquisition at 40 MHz. The cost for the Muon system upgrade is mainly driven by the number of new readout boards (Table 12). Furthermore, a certain number of muon chambers will be produced for a possible exchange as they might suffer from radiation effects. The cost of the readout system and the Low Level Trigger for adjusting the data rate at the input of the farm between 1 MHz and 40 MHz are summarized in Table 13. The TFC and ECS part of the readout system amounts to 800 kCHF and is accounted for in the detector cost.

The Common Projects consist of the online system, common electronics and the general infrastructure. The cost is detailed in Table 14. The cost of the new farm is based on 10 MHz input. The size of the farm is expected to increase progressively over the following years after 2018. The common electronics includes the cost for the fibres between patch-panels and connectors. In addition, sufficient spares for the GBT electronics, versatile links, DC-DC converters and power supplies are part of this item. Although a large fraction of the existing infrastructure will be re-used for the upgrade, almost all systems will require a modification or partial replacement. The data transmission over

detector	sub-system	countries involved
VELO	modules & infrastructure	BR, CERN, ES, IE, NL, RU, UK, US
	electronics & readout	BR, ES, CERN, CN, NL, PL, UK, US
Tracker	modules & infrastructure	CERN, CH, DE, NL, RU, UK, US
	electronics & readout	BR, CERN, CH, CN, DE, ES, FR, NL, PL, US
RICH	mechanics & infrastructure	CERN, IT, UK
	electronics & readout	CERN, IT, RO, UK
Calo	electronics & readout	ES, FR, RU
Muon	chambers	IT, RU
	electronics & readout	IT
Trigger	electronics & readout	BR, CN, FR, IT

Table 15: Expressions of interest to the detector construction, subject to funding.

optical fibres will be mandatory for all detectors and the access to the area upstream of the magnet needs to be modified. Detectors such as the Central Tracker or the Inner Tracker require new cooling systems including new piping. A large number of optical fibres will have to be pulled from the underground to the surface up to a new data center. The general and detector safety systems will be upgraded to the new conditions in the cavern. The transport team during operation consists of two staff at present and this will have to be increased to six staff during the peak period of the installation. During the installation and after moving the detectors in their final position, a survey team will measure the final position of each sub-system.

The overall cost of the LHCb upgrade varies with the choice of the sub-system technology. The core cost of the experiment including the pixel solution for the VELO and an Inner Tracker amounts to 53.4 MCHF, while a choice for the VELO strip and a Central Tracker will reduce the overall cost only slightly to 51.3 MCHF. Any other combination of technologies will stay in-between these values. For the Particle Identification system, i.e. the RICH, Calorimeter and Muon detectors, we foresee an additional reserve of 3.5 MCHF in order to account for possible modifications of some of the detector elements to comply with a luminosity of $\mathcal{L} = 2 \times 10^{33}\text{cm}^{-2}\text{s}^{-1}$. Including this reserve, the total upgrade cost amounts to 57 MCHF.

3.3 Expressions of interest

Subject to funding, Table 15 summarizes the expressions of interest of the countries in the LHCb collaboration to the construction of the different detector sub-systems, whereas Table 16 lists the participating institutes. In addition to contributing to the core detector cost, all institutes will participate with manpower and common funds to the Common Projects consisting of the Online, Common Electronics, Infrastructure and Computing. The common funds as detailed in Table 14 amount to $\sim 30\%$ of the total upgrade cost.

Code	Country	Institutes
BR	Brasil	CBPF[1], UFRL[2], PUC-Rio[3]
CERN	CERN	CERN[38]
CN	China	Tsinghua Univ.[4]
CH	Switzerland	EPFL Lausanne[39], Univ. Zürich[40]
DE	Germany	TU Dortmund[10], MPIK Heidelberg[11], Uni Heidelberg[12], Uni Rostock[13]
ES	Spain	Univ. Barcelona[36], Univ. Santiago de Compostela[37]
FR	France	CNRS/IN2P3: LAPP[5], LPC[6], CPPM[7], LAL[8], LPNHE[9]
IE	Ireland	Univ. College Dublin[14]
IT	Italy	INFN: Bari[15], Bologna[16], Cagliari[17], Ferrara[18], Firenze[19], Frascati[20], Genova[21], Milano[22], Roma Tor Vergata[23], Roma La Sapienza[24]
NL	Netherlands	Nikhef[41], VU Univ. Amsterdam[42]
PK	Pakistan	Lahore Univ.[25]
PL	Poland	Henry Niewodniczanski Inst. Krakow[26], AGH Univ. Krakow[27], Soltan Inst. Warsaw[28]
RO	Romania	Horia Hulubei Nat. Inst. Bucharest[29]
RU	Russia	PNPI[30], ITEP[31], SINP MSU[32], INR RAN[33], SB RAS Novosibirsk Univ.[34], IHEP[35]
UA	Ukraine	NSC KIPT[43], KINR[44]
UK	Great Britain	Birmingham[45], Bristol[46], Cambridge[47], Warwick[48], STFC RAL[49], Edinburgh[50], Glasgow[51], Liverpool[52], Imperial College London[53], Manchester[54], Oxford[55]
US	United States	Cincinnati[56], Syracuse[57]

Table 16: List of participating institutes, with reference to the authorlist.

References

[1] LHCb collaboration, *Letter of Intent for the LHCb Upgrade*, CERN-LHCC-2011-001, LHCC-I-018

[2] LHCb collaboration, R. Aaij *et al.*, *Strong constraints on the rare decays* $B_s^0 \to \mu^+\mu^-$ *and* $B^0 \to \mu^+\mu^-$, arXiv:1203.4493

[3] LHCb collaboration, R. Aaij *et al.*, *Differential branching fraction and angular analysis of the decay* $B^0 \to K^{*0}\mu^+\mu^-$, Phys. Rev. Lett. **108** (2012) 181806, arXiv:1112.3515

[4] LHCb collaboration, R. Aaij *et al.*, *Measurement of the CP-violating phase* ϕ_s *in the decay* $B_s^0 \to J/\psi\phi$, Phys. Rev. Lett. **108** (2012) 101803, arXiv:1112.3183

[5] LHCb collaboration, R. Aaij *et al.*, *Evidence for CP violation in time-integrated* $D^0 \to h^-h^+$ *decay rates*, Phys. Rev. Lett. **108** (2012) 111602, arXiv:1112.0938

[6] LHCb collaboration, R. Aaij *et al.*, *First evidence of direct CP violation in charmless two-body decays of* B_s^0 *mesons*, Phys. Rev. Lett. **108** (2012) 201601, arXiv:1202.6251

[7] LHCb collaboration, R. Aaij *et al.*, *Inclusive* W *and* Z *production in the forward region at* $\sqrt{s} = 7$ *TeV*, arXiv:1204.1620

[8] LHCb collaboration, R. Aaij *et al.*, and invited theorists. *Implications of LHCb measurements and future prospects*, LHCb-PUB-2012-006, in preparation

[9] LHCb collaboration, *Tagged time-dependent angular analysis of* $B_s^0 \to J/\psi\phi$ *decays at LHCb*, LHCb-CONF-2012-002

[10] LHCb collaboration, R. Aaij *et al.*, *Measurement of* ϕ_s *in* $B_s^0 \to J/\psi\pi^+\pi^-$ *decays*, arXiv:1204.5675

[11] E. Lunghi and A. Soni, *Possible evidence for the breakdown of the CKM-paradigm of CP-violation*, Phys. Lett. **B697** (2011) 323, arXiv:1010.6069

[12] LHCb collaboration, R. Aaij *et al.*, *First observation of the decay* $B_s^0 \to K^{*0}\overline{K}^{*0}$, Phys. Lett. **B709** (2012) 50, arXiv:1111.4183

[13] LHCb collaboration, R. Aaij *et al.*, *Measurement of the polarization amplitudes and triple product asymmetries in the* $B_s^0 \to \phi\phi$ *decay*, arXiv:1204.2813

[14] LHCb collaboration, *Differential branching fraction and angular analysis of the* $B^0 \to K^{*0}\mu^+\mu^-$ *decay*, LHCb-CONF-2012-008

[15] LHCb collaboration, R. Aaij *et al.*, *Measurement of the isospin asymmetry in* $B \to K^{(*)}\mu^+\mu^-$ *decays*, arXiv:1205.3422

[16] LHCb collaboration, *First observation of* $B^+ \to \pi^+\mu^+\mu^-$, LHCb-CONF-2012-006

[17] LHCb collaboration, R. Aaij *et al.*, *Observation of CP violation in* $B^+ \to DK^+$ *decays*, arXiv:1203.3662

[18] Heavy Flavour Averaging Group, D. Asner *et al.*, *Averages of b-hadron, c-hadron, and* τ*-lepton Properties*, arXiv:1010.1589, updated results and plots available at: http://www.slac.stanford.edu/xorg/hfag/

[19] CKMfitter Group, J. Charles *et al.*, *CP violation and the CKM matrix: Assessing the impact of the asymmetric B factories*, Eur. Phys. J. **C41**, (2005) 1, arXiv:hep-ph/0406184, updated results and plots available at: http://ckmfitter.in2p3.fr

[20] UTfit Collaboration, M. Bona *et al.*, *The 2004 UTfit Collaboration Report on the Status of the Unitarity Triangle in the Standard Model*, JHEP **07** (2005) 028, arXiv:hep-ph/0501199, updated results and plots available at: http://www.utfit.org/UTfit/

[21] LHCb collaboration, R. Aaij *et al.*, *Measurement of b hadron production fractions in 7 TeV pp collisions*, Phys. Rev. **D85** (2012) 032008, arXiv:1111.2357

[22] LHCb collaboration, R. Aaij *et al.*, *Observation of double charm production involving open charm in pp collisions at* $\sqrt{s}$*=7 TeV*, arXiv:1205.0975

[23] LHCb collaboration, *Search for (Higgs-like) bosons decaying into long-lived exotic particles*, LHCb-CONF-2012-014

[24] B. Schmidt, for the LHCb collaboration, *Will LHCb run in the HL-LHC era?*, Proceedings of the LHC Performance Workshop, Chamonix 2012, and references therein

[25] B. Holzer *et al.*, *Optics and Lattice optimizations for the LHC upgrade project*, Proceedings of IPAC 2012, New Orleans (Lousiana), May 2012, in preparation

[26] A. Affolder, *Charge Collection Efficiencies of Silicon Detectors after Reactor Neutron, Pion and Proton Doses up to* 2.2×10^{16} *neq* cm^{-2}, 14th RD50 Workshop on Radiation hard semiconductor devices for very high luminosity colliders, Freiburg, Germany, June 2009

[27] L. Spiegel, *A tracker/trigger design for an upgraded CMS Tracker*, Second International Conference on Technology and Instrumentation in Particle Physics, Chicago, United States, June 2011

[28] Y. Ikegami *et al.*, *R&D towards the module and service structure design for the ATLAS inner tracker at the super LHC (SLHC)*, in Proceedings of the Topical Workshop on Electronics for Particle Physics 2010 (TWEPP-10), JINST **5** (2010) C12056

[29] M. Oinonen *et al.*, *Alice Silicon Strip Detector Module Assembly with Single-Point TAB Interconnections*, in Proceedings of the 11th Workshop on Electronics for LHC and Future Experiments, Heidelberg, Germany, 12-16 Sep 2005

[30] P. Moreira *et al.*, *The GBT project*, in Proceedings of the Topical Workshop on Electronics for Particle Physics 2009 (TWEPP-09), CERN-2009-006 pp. 342-346

[31] E. Picatoste *et al.*, *Low noise front end ICECAL ASIC for the upgrade of the LHCb calorimeter*, in Proceedings of the Topical Workshop on Electronics for Particle Physics 2011 (TWEPP-11), JINST **7** (2012) C01080

[32] D. Breton and D. Charlet, *SPECS: the Serial Protocol for the Experiment Control System of LHCb*, LHCb-2003-004

[33] M. Anelli, *et al.*, *High-rate performance of the MWPCs for the LHCb Muon System*, Nucl. Instrum. Meth. **A593** (2008) 319

[34] M. Anelli, *et al.*, *High radiation tests of the MWPCs for the LHCb Muon System*, Nucl. Instrum. Meth. **A599** (2009) 171

[35] V. Suvorov, T. Schneider, B. Schmidt, W. Riegler, A. Kashchuk and D. Hutchcroft, *First results of an aging test of a full scale MWPC prototype for the LHCb Muon System*, Nucl. Instrum. Meth. **A515** (2003) 220

[36] PICMG, PICMG 3.0 Revision 3.0 AdvancedTCA Base Specification, `http://www.picmg.org`

ISBN 978-92-9083-374-1